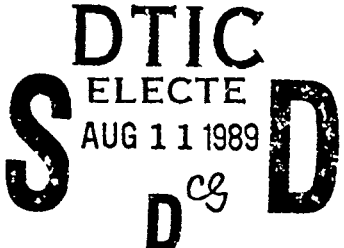


SEC

AD-A211 139

REPORT DOCUMENTATION PAGE

(2)

1a. REPORT SECURITY Unclassified		1b. RESTRICTIVE MARKINGS STK FILE COPY	
2a. SECURITY CLASSIFICATION AUTHORITY		3. DISTRIBUTION/AVAILABILITY OF REPORT Unlimited	
2b. DECLASSIFICATION/DOWNGRADING SCHEDULE			
4. PERFORMING ORGANIZATION REPORT NUMBER(S) PSU-ME-R-88/89-0067		5. MONITORING ORGANIZATION REPORT NUMBER(S) AFOSR-TR. 89-1059	
6a. NAME OF PERFORMING ORGANIZATION The Pennsylvania State University		6b. OFFICE SYMBOL (If applicable) —	
6c. ADDRESS (City, State, and ZIP Code) Department of Mechanical Engineering University Park, PA 16802		7a. NAME OF MONITORING ORGANIZATION Air Force Office of Scientific Research	
7b. ADDRESS (City, State, and ZIP Code) AFOSR/NA, Bldg 410 Bolling AFB, DC 20332-6448			
8a. NAME OF FUNDING/SPONSORING ORGANIZATION Air Force Office of Scientific Research		8b. OFFICE SYMBOL (If applicable) NA	
8c. ADDRESS (City, State, and ZIP Code) AFOSR/NA, Bldg 410 Bolling AFB DC 20332-6448		9. PROCUREMENT INSTRUMENT IDENTIFICATION NUMBER AFOSR-87-0142	
10. SOURCE OF FUNDING NUMBERS			
		PROGRAM ELEMENT NO. 61102F	PROJECT NO. 2302
		TASK NO. SI	WORK UNIT ACCESSION NO.
11. TITLE (Include Security Classification) Analytical Study of Mistuning/Friction/Aerodynamics Interaction in a Bladed Disk Assembly			
12. PERSONAL AUTHOR(S) Sinha, A. and Chen, S.			
13a. TYPE OF REPORT Final	13b. TIME COVERED FROM 5/87 TO 1/89		14. DATE OF REPORT (Year, Month, Day) 89/06/02
15. PAGE COUNT 74			
16. SUPPLEMENTARY NOTATION			
17. COSATI CODES		18. SUBJECT TERMS (Continue on reverse if necessary and identify by block number) Mistuning, probability density functions of amplitudes, efficient analytical technique	
FIELD	GROUP	SUB-GROUP	
19. ABSTRACT (Continue on reverse if necessary and identify by block number)			
<p>PLEASE SEE REVERSE SIDE</p> <p style="text-align: center;">  DTIC ELECTE AUG 11 1989 S D <i>CG</i> </p> <p style="text-align: center;">89 8 10 065</p>			
20. DISTRIBUTION/AVAILABILITY OF ABSTRACT <input checked="" type="checkbox"/> UNCLASSIFIED/UNLIMITED <input type="checkbox"/> SAME AS RPT		21. ABSTRACT SECURITY CLASSIFICATION UNCLASSIFIED	
22a. NAME OF RESPONSIBLE INDIVIDUAL Dr Anthony K. Amos		22b. TELEPHONE (Include Area Code) 1203 707-4937	22c. OFFICE SYMBOL NA

ABSTRACT

First, the analytical technique is shown to be valid for the computation of the statistics of a blade's vibratory amplitude when the distributions of modal parameters of a mistuned bladed disk assembly are non-Gaussian. The results from the analytical technique are compared with those from numerical simulations for triangular and uniform distributions. It has been found that the probability density function of the amplitude is insensitive to the types of mistuning distributions.

Second, an analytical technique has been developed to efficiently compute the probability density function of the maximum amplitude on a mistuned bladed disk assembly. This technique uses the direct Taylor series expansion in terms of the perturbation in an amplitude as a function of perturbations in modal stiffnesses. The validity of the technique has been corroborated by comparison with the results from numerical simulations.

Lastly, the statistics of the forced response of a structurally and aerodynamically coupled bladed disk assembly have been computed efficiently by the analytical technique. The results from the analytical technique agree well with those from numerical simulations. The effects of the following parameters on the statistics of the maximum amplitude have been studied: the aerodynamic couplings among blades, the fluid density and the cascade stagger angle.

AFOSR-TR- 89-1059

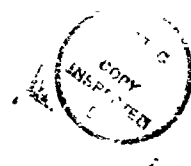
ANALYTICAL STUDY OF MISTUNING/FRICTION/AERODYNAMICS
INTERACTION IN A BLADED DISK ASSEMBLY

FINAL REPORT
AFOSR GRANT #87-0142

Principal Investigator: Dr. Alok Sinha
Graduate Student: Shing Chen

Department of Mechanical Engineering
The Pennsylvania State University
University Park, PA 16802

Accession For	
NTIS CRA&I	<input checked="" type="checkbox"/>
DTIC TAB	<input type="checkbox"/>
Unannounced	<input type="checkbox"/>
Justification	
By	
Distribution	
Availability Codes	
Dist	Avail. and/or Special
A-1	



ABSTRACT

First, the analytical technique is shown to be valid for the computation of the statistics of a blade's vibratory amplitude when the distributions of modal parameters of a mistuned bladed disk assembly are non-Gaussian. The results from the analytical technique are compared with those from numerical simulations for triangular and uniform distributions. It has been found that the probability density function of the amplitude is insensitive to the types of mistuning distributions.

Second, an analytical technique has been developed to efficiently compute the probability density function of the maximum amplitude on a mistuned bladed disk assembly. This technique uses the direct Taylor series expansion in terms of the perturbation in an amplitude as a function of perturbations in modal stiffnesses. The validity of the technique has been corroborated by comparison with the results from numerical simulations.

Lastly, the statistics of the forced response of a structurally and aerodynamically coupled bladed disk assembly have been computed efficiently by the analytical technique. The results from the analytical technique agree well with those from numerical simulations. The effects of the following parameters on the statistics of the maximum amplitude have been studied: the aerodynamic couplings among blades, the fluid density and the cascade stagger angle.

CONTENTS

SECTION 1 (pages 1 to 33)

"Probabilistic Analysis of Forced Response of a Bladed Disk Assembly with Various Mistuning Distributions".

SECTION 2 (pages 34 to 56)

"Calculating the Statistics of the Maximum Amplitude of a Mistuned Bladed Disk Assembly".

SECTION 3 (pages 57 to 74)

"Analytical Statistics of Forced Response of a Mistuned Bladed Disk Assembly in Subsonic Flow".

SECTION 1

**PROBABILISTIC ANALYSIS OF FORCED RESPONSE OF A PLADED
DISK ASSEMBLY WITH VARIOUS MISTUNING DISTRIBUTIONS**

ABSTRACT

In this paper, efficient algorithms have been developed to compute the statistics of forced response of a mistuned bladed disk assembly. The technique is valid for Gaussian and non-Gaussian distributions of modal parameters as well. The validity of this technique is shown by comparison with results from numerical simulations for triangular and uniform distributions. The results for Gaussian, triangular and uniform distributions indicate that the cumulative probability density function of a blade's amplitude primarily depends on the standard deviations of modal parameters rather than on the type of distributions.

NOMENCLATURE

A_j	amplitude of the j th mass (mistuned system)
a_{ij}	elements of matrix H^{-1}
B	amplitude of each blade in tuned system
c	damping coefficient
$E()$	expected value
f	external force vector
$g_1(), g_2()$	probability density function
H	matrix with elements composed of m_t , k_t , c and ω
H_c	complex matrix corresponding to H
i	$\sqrt{-1}$
I	identity matrix
k_t	modal stiffness of each blade (tuned system)
m_t	modal mass of each blade (tuned system)

N	number of blades
NS	number of simulations
r	order of engine excitation
R	λ/k_t
U	vector defined by Eq. (10)
u_j	jth element of U
V	vector defined by Eq. (11)
v_j	jth element of V
X	response vector (mistuned system)
x_t	response vector (tuned system)
γ_j	correlation coefficient between u_{2j} and u_{2j-1}
ζ	damping factor ($-c/(2m_t \omega)$ for resonance condition)
δA_j	amplitude of δx_j
δX	$X - x_t$
δx_j	jth element of δX
$\delta \phi_j$	phase of δx_j
λ	standard deviation of δk_j
σ_j	standard deviation of u_j
ϕ_j	phase of x_j
ω	excitation frequency

1. Introduction

Mistuning refers to variation in modal properties of blades which is caused by minor differences in their geometries that arise during the manufacturing process. It has received wide attention in the existing literature [1,2] because even a small amount of mistuning can lead to a

large variation in the blade's amplitudes within the same assembly. In fact, the amplitude of vibration of the worst blade may often be as high as two times the amplitude of a blade of a perfectly tuned system. Since the deviations of modal properties of blades from their nominal values are randomly distributed, it is important for the designer to predict the statistics of forced response, particularly the probability that the maximum amplitude on any disk would exceed a critical value, in a computationally efficient manner. For this purpose, an efficient computational technique has been presented by the authors in their earlier papers [3-4] where the distributions of modal parameters are assumed to be Gaussian. In this paper, the analytical technique is extended to include non-Gaussian distributions. Also, an efficient algorithm has been developed to invert the tuned system matrix which further reduces the computation time.

The distributions of modal parameters are often assumed to be Gaussian for the sake of analytical simplicity. However, in practice, they may not be Gaussian. Therefore, the following issue arises: does one type of distributions of modal parameters leads to worse scatter in amplitudes than another? This issue has been addressed in this paper by studying the distributions of amplitudes for three types of distributions of modal parameters with the same standard deviations: Gaussian, uniform and triangular. It is found that the cumulative probability distribution functions of a blade's amplitude is almost identical for these three types of parameters' distributions.

The model of bladed disk assembly is chosen to be as shown in Figure 1. Even though it is a simple model, it contains all the basic characteristics of a bladed disk assembly and has been used by the authors in their previous papers [3-5]. In Figure 1, m_t and k_j are the modal mass and stiffness of each blade, respectively. The phenomenon of mistuning is simulated by considering k_j as a random variable. The stiffness k_C represents the coupling between adjacent blades due to disk's flexibility.

First, the technique for the efficient computation of the statistics of forced response is described. The accuracy of this technique is then studied for triangular and uniform distributions by comparison with results from numerical simulations. Lastly, the values of probability that a blade's amplitude exceeds certain critical value are examined as a function of excitation frequency for Gaussian, triangular and uniform distributions of k_j .

2. Computation of Statistics of Forced Response

The computational technique is presented for the system shown in Figure 1. However, it can be directly applied to a more complex spring-mass model of a bladed disk assembly; e.g., the model developed by Griffin and Hoosac [6].

The system of differential equations governing the dynamics of a mistuned bladed disk model depicted in Figure 1 is described as follows:

$$m_t \ddot{x}_j + k_j x_j + k_C(x_j - x_{j+1}) + k_C(x_j - x_{j-1}) + c \dot{x}_j = f_0 \cos(\omega t + \psi_j); \quad j=1, 2, \dots, N \quad (1)$$

where N is the number of blades. The excitation phase ψ_j is defined for a r th engine order excitation as follows:

$$\psi_j = 2\pi r(j-1)/N; \quad r = 0, 1, 2, \dots, N-1 \quad (2)$$

Represent

$$k_j = k_t + \delta k_j \quad (3)$$

where k_t is the stiffness of the perfectly tuned system. The deviation δk_j is taken to be a random variable with zero mean; i.e., $E(\delta k_j) = 0$. Also, the distribution of δk_p is assumed to be independent of $\delta k_j (p \neq j)$. It should be noted that there is no assumption made on the nature of the distribution of δk_j .

Now the response (x_{tj}) of the tuned system satisfies the following equation:

$$\begin{aligned} m_t \ddot{x}_{tj} + k_t x_{tj} + kC(x_{tj} - x_{t(j+1)}) + kC(x_{tj} - x_{t(j-1)}) \\ + c \dot{x}_{tj} = f_0 \cos(\omega t + \psi_j) \end{aligned} \quad (4)$$

Subtracting (4) from (1),

$$\begin{aligned} m_t \ddot{\delta x}_j + (k_t + \delta k_j) \delta x_j + kC(\delta x_j - \delta x_{j+1}) + kC(\delta x_j - \delta x_{j-1}) \\ + c \dot{\delta x}_j = -\delta k_j x_{tj} \end{aligned} \quad (5)$$

where $\delta x_j = x_j - x_{tj}$.

In steady state, the response x_j and x_{tj} are sinusoidal. Therefore, δx_j would also be sinusoidal. Let

$$x_j = A_j \cos(\omega t + \phi_j) \quad (6)$$

$$x_{tj} = B \cos(\omega t + \theta_j) \quad (7)$$

and

$$\delta x_j = \delta A_j \cos(\omega t + \delta \phi_j) \quad (8)$$

Substituting (7) and (8) into (5) and then equating the coefficients of $\cos \omega t$ and $\sin \omega t$ on both sides, the following system of $2N$ algebraic equations is obtained:

$$(H + \delta H)U = -\delta HV \quad (9)$$

where

$$U = [\delta A_1 \cos \delta \phi_1 \quad \delta A_1 \sin \delta \phi_1 \quad \dots \quad \delta A_N \cos \delta \phi_N \quad \delta A_N \sin \delta \phi_N]^T \quad (10)$$

$$V = [B \cos \theta_1 \quad B \sin \theta_1 \quad \dots \quad B \cos \theta_N \quad B \sin \theta_N]^T \quad (11)$$

The matrices H and δH are defined in the Appendix A. Since the matrix H is non-singular for a damped system, the equation (9) yields

$$\begin{aligned} U &= -(I + H^{-1} \delta H)^{-1} H^{-1} \delta H V \\ &= -(H^{-1} \delta H - (H^{-1} \delta H)^2 + (H^{-1} \delta H)^3 - \dots) V \end{aligned} \quad (12)$$

Therefore, the expression for each element of the vector U has the following form.

$$u_p = - \sum_{j=1}^N t_{p,j} \delta k_j + \sum_{j=1}^N \sum_{s=1}^N w_{p,j,s} \delta k_j \delta k_s - \sum_{j=1}^N \sum_{s=1}^N \sum_{l=1}^N y_{p,j,s,l} \delta k_j \delta k_s \delta k_l + \dots \quad (13)$$

where

$$t_{p,j} = a_{p,2j-1} v_{2j-1} + a_{p,2j} v_{2j} \quad (14)$$

$$w_{p,j,s} = a_{p,2j-1} t_{2j-1,s} + a_{p,2j} t_{2j,s} \quad (15)$$

$$y_{p,j,s,l} = a_{p,2j-1} w_{2j-1,s,l} + a_{p,2j} w_{2j,s,l} \quad (16)$$

$$a_{p,j} = (H^{-1})_{p,j} \quad (17)$$

An efficient algorithm has been outlined in Appendix B for the inversion of matrix H . Therefore, all the coefficients in (13) can be computed in an efficient manner.

The equation (13) indicates that each u_p is a linear combination of a large number of random variables which are not highly dependent [4]. Therefore, the central limit theorem [7] indicates that the distribution of u_p can be approximated to be Gaussian.

The number of terms in the series expansion (12) which make significant contributions depends on the value of R/ζ where $R = \sqrt{E(\delta k_j^2)}/k_t$ and ζ is the damping factor. When R/ζ is small, the higher-order terms in (13) can be neglected and u_p can be expressed as

$$u_p = - \sum_{j=1}^N t_{p,j} \delta k_j \quad (18)$$

When the distribution of δk_j is Gaussian, the distribution of u_p is exactly Gaussian for any number of blades [3]. However, for non-Gaussian δk_j , the distribution of u_p can be approximated to be Gaussian only for a large value of N .

Using central limit theorem, the distribution of ϵ ($= \eta u_{2j-1} + \mu u_{2j}$) can also be approximated to be Gaussian for any η and μ . Therefore, u_{2j-1} and u_{2j} can be described as jointly Gaussian [8], i.e.,

$$g_1(u_{2j-1}, u_{2j}) =$$

$$\frac{1}{2\pi\sigma_{2j-1}\sigma_{2j}(1-\gamma_j^2)^{1/2}} \exp \left\{ -\frac{1}{2(1-\gamma_j^2)} \left[\frac{\alpha^2}{\sigma_{2j-1}^2} - \frac{2\gamma_j\alpha\beta}{\sigma_{2j-1}\sigma_{2j}} + \frac{\beta^2}{\sigma_{2j}^2} \right] \right\} \quad (19)$$

where

$$\alpha = u_{2j-1} - E(u_{2j-1})$$

$$\beta = u_{2j} - E(u_{2j})$$

$$\sigma_r^2 = E(u_r^2) - (E(u_r))^2$$

$$\gamma_j = (E(u_{2j-1}u_{2j}) - E(u_{2j-1})E(u_{2j})) / (\sigma_{2j-1} \cdot \sigma_{2j})$$

From (19), the probability density function of a blade's amplitude can be calculated as

$$g_2(A_j) = \frac{A_j}{2\pi\sigma_{2j-1}\sigma_{2j}\sqrt{1-\gamma_j^2}} \int_0^{2\pi} \exp\left[-\frac{Z(v)}{2(1-\gamma_j^2)}\right] dv \quad (20)$$

where

$$Z(v) = \frac{(A_j \cos v - \alpha_1)^2}{\sigma_{2j-1}^2} - \frac{2\gamma_j (A_j \cos v - \alpha_1) (A_j \sin v - \beta_1)}{\sigma_{2j-1} \sigma_{2j}}$$

$$+ \frac{(A_j \sin v - \beta_1)^2}{\sigma_{2j}^2}$$

$$\alpha_1 = v_{2j-1} + E(u_{2j-1})$$

$$\beta_1 = v_{2j} + E(u_{2j})$$

The probability, Pr , that A_j will be less than a critical value, A_c , can be calculated using (20) as follows;

$$Pr(A_j < A_c) = \frac{\int_0^{A_c} g_2(A_j) dA_j}{\int_0^{\infty} g_2(A_j) dA_j} \quad (21)$$

It should be noted that the mean and variance of u_p can be calculated without performing numerical simulations. However, the number of terms in (13) which would yield accurate results has to be determined. In this paper, $E(u_p)$ and $E(u_p^2)$ are computed (Appendix III) on the basis of first three terms in (13) for three types of distributions for δk_j : Gaussian [4], uniform and triangular. It has been found that the results are fairly accurate at a realistic value of R/ζ .

3. Results and Discussions

3.1 Accuracy of the Analytical Technique for Non-Gaussian Distributions

In order to verify the accuracy of the analytical technique for non-Gaussian distributions of modal stiffness δk_j , the results from numerical simulations are compared to those obtained analytically. Two types of distributions, triangular (Figure 2) and uniform (Figure 3), are considered primarily because they can be conveniently generated using IMSL subroutines [9] GGTRA and GGUBS for numerical simulations. These IMSL subroutines are used to choose the modal stiffness of each blade from populations with specified mean and variance. The response of the resulting bladed disk assembly is obtained by solving the linear system of

algebraic equations [3] in terms of $A_j \cos\phi_j$ and $A_j \sin\phi_j$. The statistics of $A_j \cos\phi_j$, $A_j \sin\phi_j$ and A_j are then generated by considering a large number (arbitrarily chosen to be 500) of bladed disk assemblies with different sets of blades' modal stiffnesses.

The nominal values of modal parameters are chosen from the paper by Griffin and Sinha [5] and are presented in Table 1. The number of blades is selected to be twenty four. The excitation frequency ω is chosen to represent resonance condition. The standard deviation (λ) of each blade is taken to be 8,000. At this value of λ , the ratio of standard deviation and mean value of individual blade's natural frequency is found to be 0.0096 which represents the typical value found in practice. The damping coefficient c is chosen to be 1.443. This value of damping corresponds to about 1% damping factor which is typically observed in engines from aerodynamic and structural sources.

The results for triangular distribution are presented in Figures 4-6 for third engine order excitation. The distributions of $A_j \cos\phi_j$ and $A_j \sin\phi_j$, obtained from numerical simulations, are examined for each blade. Each of these distributions is compared to the Gaussian distribution with same mean and variance; e.g., Figures 4 and 5. The chi-square test of hypothesis [10] indicates that the distributions of $A_j \cos\phi_j$ and $A_j \sin\phi_j$ are Gaussian, which confirms the applicability of central limit theorem. The distributions of amplitudes, obtained from eq. (20), are then compared to those from numerical simulations; e.g., Figure 6. The chi-square test of hypothesis again indicates that the probability density function of amplitude predicted by the analytical technique is accurate.

Next the results for uniform distribution are presented in figure 7-9. Again, the distributions of $A_j \cos\phi_j$ and $A_j \sin\phi_j$ are found to be Gaussian, Figures 7 and 8. Also, the probability distribution functions of amplitudes, obtained from eq. (20), compare well with those from numerical simulations; e.g., Figure 9.

3.2 Probability That The Amplitude is Greater Than A Critical Value

Using the equation (21), the probability (Pr) that a blade's amplitude exceeds a critical value can be easily calculated. Assuming that the critical value of the amplitude is $1.4B$, the values of Pr are shown in Figure 10 as a function of excitation frequencies for all the three types of distributions of δk_j and three different engine order excitations. It is found that the maximum value of Pr for each engine order excitation occurs at a frequency which is slightly below the corresponding undamped natural frequency. Also, the values of Pr are almost identical for three different distributions of δk_j . These results indicate that the probability that the amplitude would exceed a certain value depends primarily on the standard deviation of δk_j ; e.g. Figure 11.

4. Conclusions

In this paper, the analytical technique developed in [4] is shown to be valid for non-Gaussian distributions of modal parameters. This technique provides the probability distribution function of each blade; i.e., the probability that a blade's amplitude is greater than a certain critical value can be easily calculated. The validity of this technique is established by comparison with results from numerical simulations for

triangular and uniform distributions of blades' modal stiffnesses. Even though the analytical technique is presented for a simple bladed disk assembly (Figure 1), it can be directly applied to a more complex spring-mass model of a bladed disk assembly; e.g., the model used in [6]. Also, an efficient algorithm which uses fast Fourier transform has been developed to invert the tuned system matrix which further reduces the computation time.

The values of probability that an amplitude is greater than a certain critical value are found to be almost identical for Gaussian, uniform and triangular distributions of modal stiffness with the same values for standard deviations. In other words, the cumulative probability density function of a blade's amplitude depends primarily on the standard deviation of modal stiffness.

5. Acknowledgement

This work has been supported by AFOSR Grant 87-0142 under the direction of Dr. Anthony K. Amos.

REFERENCES

1. Ewins, D. J. and Srinivasan, A. V. (Editors), Vibration of Bladed Disk Assemblies, ASME, New York, 1983.
2. Kielb, R. E. and Reiger, N. F. (Editors), Vibration of Blades and Bladed Disk Assemblies, ASME, New York, 1985.
3. Sinha, A., "Calculacing the Statistics of Forced Response of a Mistuned Bladed Disk Assembly," AIAA Journal, Vol. 24, No. 11, 1986, pp. 1797-1801.
4. Sinha, A. and Chen, S., "A Higher-Order Technique to Compute the Statistics of Forced Response of a Mistuned Bladed Disk Assembly," submitted to Journal of Sound and Vibration.
5. Griffin, J. H. and Sinha, A., "The Interaction Between Mistuning and Friction in the Forced Response of Bladed Disk Assemblies," ASME Journal of Engineering for Gas Turbines and Power, Vol. 107, January 1985, pp. 205-211.
6. Griffin, J. H. and Hoosac, T. M., "Model Development and Statistical Investigation of Turbine Blade Mistuning," ASME Journal of Vibration, Acoustics, Stress and Reliability in Design, Vol. 106, April 1984.
7. Benjamin, J. R. and Cornell, C. A., Probability, Statistics and Decision for Civil Engineers, McGraw-Hill Book Company, New York, 1970, pp. 251-253.
8. Papoulis, A., Probability, Random Variables and Stochastic Processes, McGraw-Hill Book Company, New York, 1965.
9. IMSL Reference Manual, IMSL Inc., Houston, TX 1984.
10. Spiegel, M. R., "Theory and Problems of Probability and Statistics," Schaum's Outline Series, McGraw-Hill Book Company, New York, 1975.
11. Oppenheim, A. V., and Schafer, R. W., Digital Signal Processing, Prentice-Hall, Inc., New Jersey, 1975.

Appendix A
Matrices H and δH

$H =$

$$\begin{bmatrix} h_1 & h_3 & -h_2 & 0 & 0 & 0 & \dots & \dots & -h_2 & 0 \\ -h_3 & h_1 & 0 & -h_2 & -h_2 & 0 & \dots & \dots & 0 & -h_2 \\ -h_2 & 0 & h_1 & h_3 & -h_2 & 0 & \dots & \dots & 0 & 0 \\ 0 & -h_2 & -h_3 & h_1 & 0 & -h_2 & \dots & \dots & 0 & 0 \\ & & & & & & & & & \\ -h_2 & 0 & 0 & 0 & 0 & 0 & \dots & \dots & h_1 & h_3 \\ 0 & -h_2 & 0 & 0 & 0 & 0 & \dots & \dots & -h_3 & h_1 \end{bmatrix}$$

(A-1)

where

$$h_1 = k_t + 2kC - m_t\omega^2, \quad h_2 = kC, \quad h_3 = -c\omega$$

$\delta H =$

$$\begin{bmatrix} \delta k_1 & & & & & & & \\ & \delta k_1 & & & & & & \\ & & \delta k_2 & & & & & \\ & & & \delta k_2 & & & & \\ & & & & \ddots & & & \\ & & & & & \ddots & & \\ & & & & & & \delta k_N & \\ & & & & & & & \delta k_N \end{bmatrix}$$

(A-2)

Appendix B
Inversion of Matrix H

It can be seen from eq. (A-1) that the matrix H corresponds to a perfectly tuned system and is circular in nature. In order to obtain an efficient technique to determine H^{-1} , it is convenient to use complex excitation; i.e., the differential equation for the tuned system is written as follows

$$\begin{aligned} m_t \ddot{x}_{tj} + k_t \dot{x}_{tj} + kC(x_{tj} - x_{t(j+1)}) + kC(x_{tj} - x_{t(j-1)}) \\ + c \dot{x}_{tj} = f_0 e^{i(\omega t + \psi_j)} \end{aligned} \quad (B-1)$$

The steady-state response x_{tj} can be represented as follows:

$$x_{tj} = A_j^* e^{i\omega t} \quad (B-2)$$

Substituting (B-2) into (B-1) and equating the coefficients of $e^{i\omega t}$ on both sides, the following system of N algebraic equations is obtained:

$$H_{c-r} A^* = f_r \quad (B-3)$$

where

$$H_c = \begin{matrix} kk & -kC & 0 & \dots & \dots & -kC \\ -kC & kk & -kC & \dots & \dots & 0 \\ \cdot & \cdot & \cdot & \ddots & & \cdot \\ \cdot & \cdot & \cdot & \ddots & & \cdot \\ \cdot & \cdot & \cdot & \ddots & & \cdot \\ -kC & 0 & \dots & \dots & \dots & kk \end{matrix} \quad (B-4)$$

$$kk = (k_t + 2kc - m_t\omega^2) + ic\omega$$

$$\underline{A^*}_r = [A^*_{1,r} \ A^*_{2,r} \ \dots \ \dots \ \dots \ A^*_{N,r}]^T \quad (B-5)$$

$$\underline{f}_r^* = f_0 [e^{i\psi_1} \ e^{i\psi_2} \ \dots \ \dots \ \dots \ e^{i\psi_N}]^T \quad (B-6)$$

For the r th engine-order excitation,

$$\psi_j = 2\pi r(j-1)/N \quad (B-7)$$

From (B-3),

$$\underline{A}_r^* = H_c^{-1} \underline{f}_r \quad (B-8)$$

Representing

$$(H_c^{-1})_{p,j} = a_{p,j}^* \quad (B-9)$$

and using (B-6), (B-7) and (B-8),

$$A_{1,r}^* = \sum_{l=1}^N a_{1,l}^* e^{i2\pi r(l-1)/N}; \quad r = 0, 1, 2, \dots, N-1 \quad (B-10)$$

The equation (B-10) indicates that $A_{1,r}^*$ is discrete Fourier transform [11] of $a_{1,l}^*$. Therefore,

$$a_{1,l}^* = \frac{1}{N} \sum_{r=0}^{N-1} A_{1,r}^* e^{-i2\pi r(l-1)/N}; \quad l = 1, 2, \dots, N \quad (B-11)$$

For each engine-order excitation, $A^*_{1,r}$ can be computed [3] by analyzing an equivalent single-degree of freedom system and is given by

$$A^*_{1,r} = \frac{(k_e - \omega^2 m_t) f_0}{(k_e - \omega^2 m_t)^2 + c^2 \omega^2} - i \frac{c \omega f_0}{(k_e - \omega^2 m_t)^2 + c^2 \omega^2} \quad (B-12)$$

where

$$k_e = k_t + 4kC \sin^2(\pi r/N).$$

Having obtained $A^*_{1,r}$, the first row ($a^*_{1,l}$) of H_C^{-1} matrix can be obtained from (B-11) using a Fast Fourier transform (FFT) algorithm [11] which is computationally efficient.

Now for the elements of p th row of H_C^{-1} matrix,

$$a^*_{p,l} = \frac{1}{N} \sum_{r=0}^{N-1} A^*_{p,r} e^{-i2\pi(r-1)/N} \quad (B-13)$$

Since

$$A^*_{p,r} = A^*_{1,r} e^{i2\pi(p-1)/N}, \quad (B-14)$$

it can be seen that

$$a^*_{p,l} = a^*_{1,(l-p+1)} \quad (B-15)$$

Furthermore, it can be derived from (B-11) that

$$a^*_{1,-q} = a^*_{1,(N-q)} \quad (B-16)$$

The equations (B-15) and (B-16) indicate that H_C^{-1} is also a circular matrix, and hence the computation of its first row is sufficient to determine all the elements of H_C^{-1} .

Lastly, it can be easily verified that

$$a_{2p-1,2j-1} = a_{2p,2j} = \text{Real}(a^*_{pj}) \quad (B-17)$$

$$-a_{2p-1,2j} = a_{2p,2j-1} = \text{Imag}(a^*_{pj}) \quad (B-18)$$

where

$$a_{p,j} = (H^{-1})_{p,j}$$

In summary, H_C^{-1} is obtained by computing the steady state response of the equivalent single degree of freedom model for each engine order excitation. If each blade sector is represented by a greater number of degrees of freedom; e.g., three in [6], the dimensions of matrix H_C will be $3N \times 3N$. In this case, the inversion of matrix H_C will involve the computation of the steady state response of the equivalent three degrees of freedom system for each engine order excitation. In other words, N number of 3×3 matrices have to be inverted. This approach results in a significant reduction in computing time with respect to that required for direct inversion of a $3N \times 3N$ matrix, particularly when N is large.

Appendix C

Computation of $E(u_p)$ and $E(u_p^2)$

In the previous paper [4], formulae for computing $E(u_p)$ and $E(u_p^2)$ have been developed when the distributions of δk_j are Gaussian. Here, these formulae are generalized to include the cases of uniform and triangular distributions of δk_j .

First, the following results are derived for triangular (Figure 2) and uniform distributions (Figure 3):

$$0 \quad ; \quad \text{for odd } n$$

$$E(\delta k_j^n) = \frac{2\lambda^n 6^{n/2}}{(n+1)(n+2)}; \quad \text{for even } n \text{ and triangular distribution} \quad (C-1)$$

$$\frac{\lambda^n 3^{n/2}}{(n+1)}; \quad \text{for even } n \text{ and uniform distributions}$$

where

$$E(\delta k_j^2) = \lambda^2 \quad (C-2)$$

Second, it is recalled that the distribution of δk_j is independent of that $\delta k_s (j \neq s)$. Therefore,

$$E(\delta k_j^l \delta k_s^p) = E(\delta k_j^l) E(\delta k_s^p) \quad (C-3)$$

Analogous to expressions in [4], $E(u_p)$ is computed on the basis of first three terms in (13) and $E(u_p u_q)$ only on the basis of terms up to δk_j^4 (or $\delta k_j^2 \delta k_s^2$).

Hence, using (C-1) and (C-3), the following expressions are obtained for computing $E(u_p)$ and $E(u_p u_q)$:

$$E(u_p) = \lambda^2 \sum_{j=1}^N w_{p,j,j} \quad (C-4)$$

$$E(u_p u_q) = \lambda^2 \sum_{j=1}^N t_{p,j} t_{q,j}$$

$$+ [\beta \sum_{j=1}^N y_{q,j,j,j} t_{p,j} + \sum_{j=1}^N \sum_{\substack{l=1 \\ j \neq l}}^N t_{p,l} (y_{q,j,j,l} + y_{q,j,l,j} + y_{q,l,j,j})] \lambda^4$$

$$+ [\beta \sum_{j=1}^N y_{p,j,j,j} t_{q,j} + \sum_{j=1}^N \sum_{\substack{l=1 \\ j \neq l}}^N t_{q,l} (y_{p,j,j,l} + y_{p,j,l,j} + y_{p,l,j,j})] \lambda^4$$

$$+ [\beta \sum_{j=1}^N w_{p,j,j} w_{q,j,j} + \sum_{j=1}^N \sum_{\substack{l=1 \\ j \neq l}}^N w_{p,j,j} w_{q,l,l} + w_{p,j,l} (w_{q,j,l} + w_{q,l,j})] \lambda^4 \quad (C-5)$$

where

3.0 for Gaussian δk_j

$\beta = 2.4$ for triangular δk_j (C-6)

1.8 for uniform δk_j

It is obvious that $E(u_p^2)$ can also be computed from (C-5) by substituting $q=p$.

TABLE 1. System Parameters (SI units) $m_t = 0.0114$ $k_t = 430000.$ $kC = 45430.$

LIST OF FIGURES

Figure 1: Model of Bladed Disk Assembly

Figure 2: Triangular Distribution of δk_j

Figure 3: Uniform Distribution of δk_j

Figure 4: Distributions of $A_j \cos \phi_j$ (Triangular Distribution of δk_j)

Figure 5: Distributions of $A_j \sin \phi_j$ (Triangular Distribution of δk_j)

Figure 6: Distributions of A_j (Triangular Distribution of δk_j)

Figure 7: Distributions of $A_j \cos \phi_j$ (Uniform Distribution of δk_j)

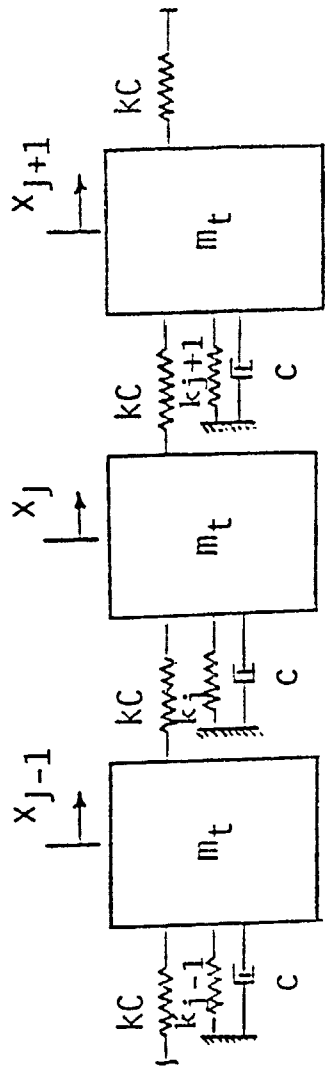
Figure 8: Distributions of $A_j \sin \phi_j$ (Uniform Distribution of δk_j)

Figure 9: Distributions of A_j (Uniform Distribution of δk_j)

Figure 10: Probability of $A_j > 1.4 B$ vs. Excitation Frequency

Figure 11: Cumulative Probability

Figure 1
Sinha & Chen



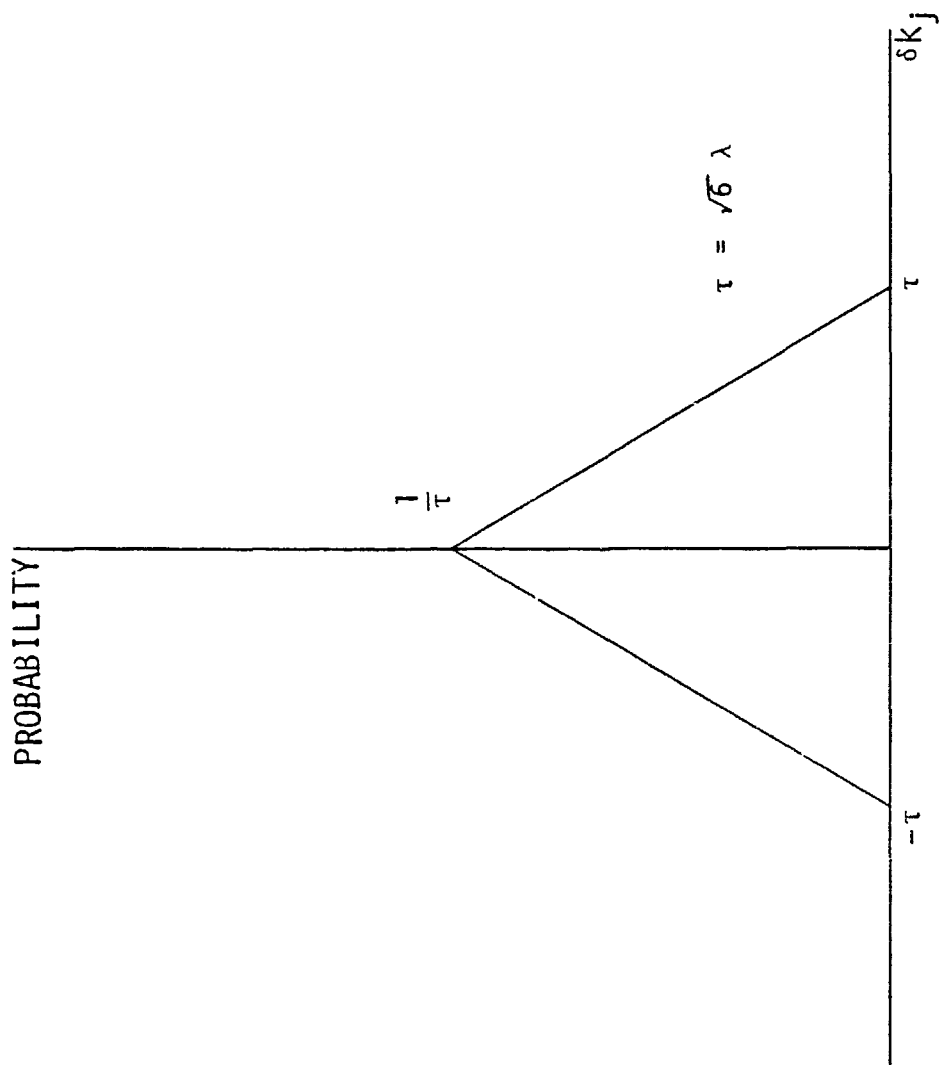


Figure 3²⁵
Sinha + Che

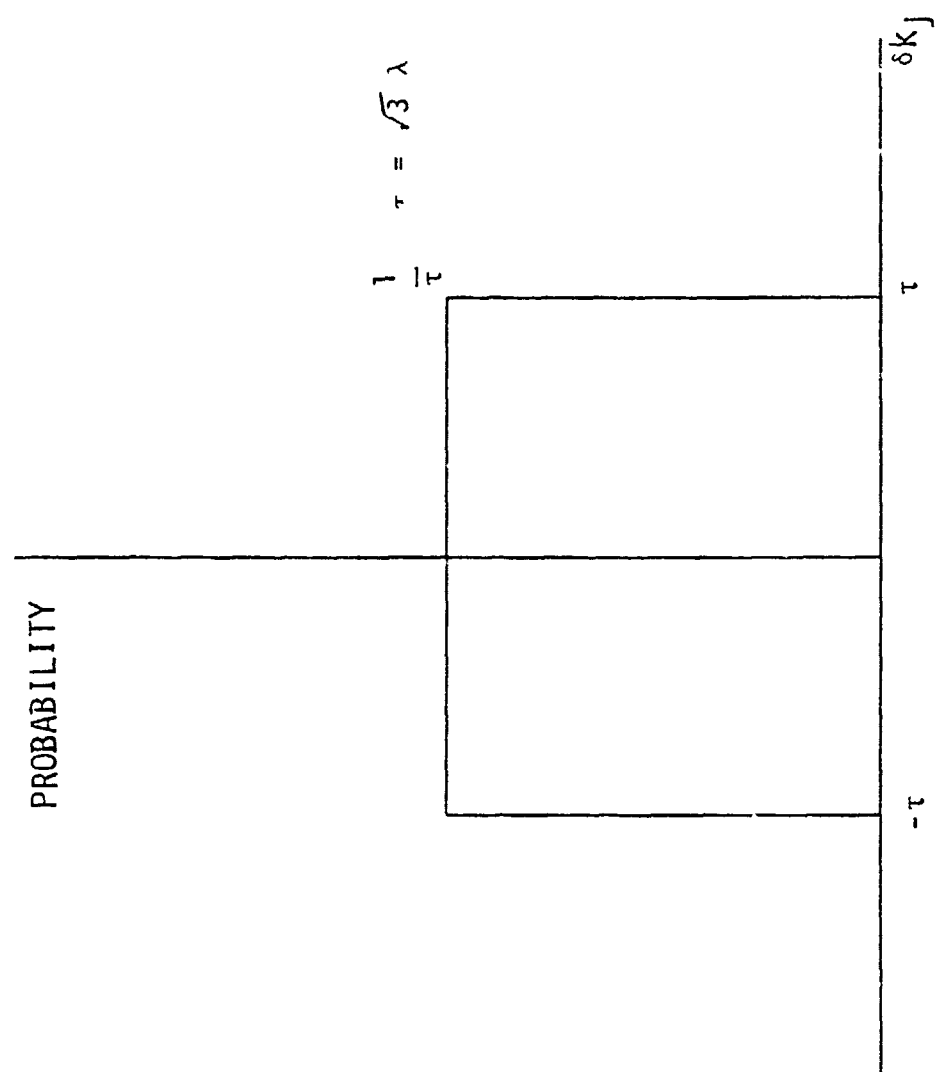


Figure 4
Sinha & Cie.

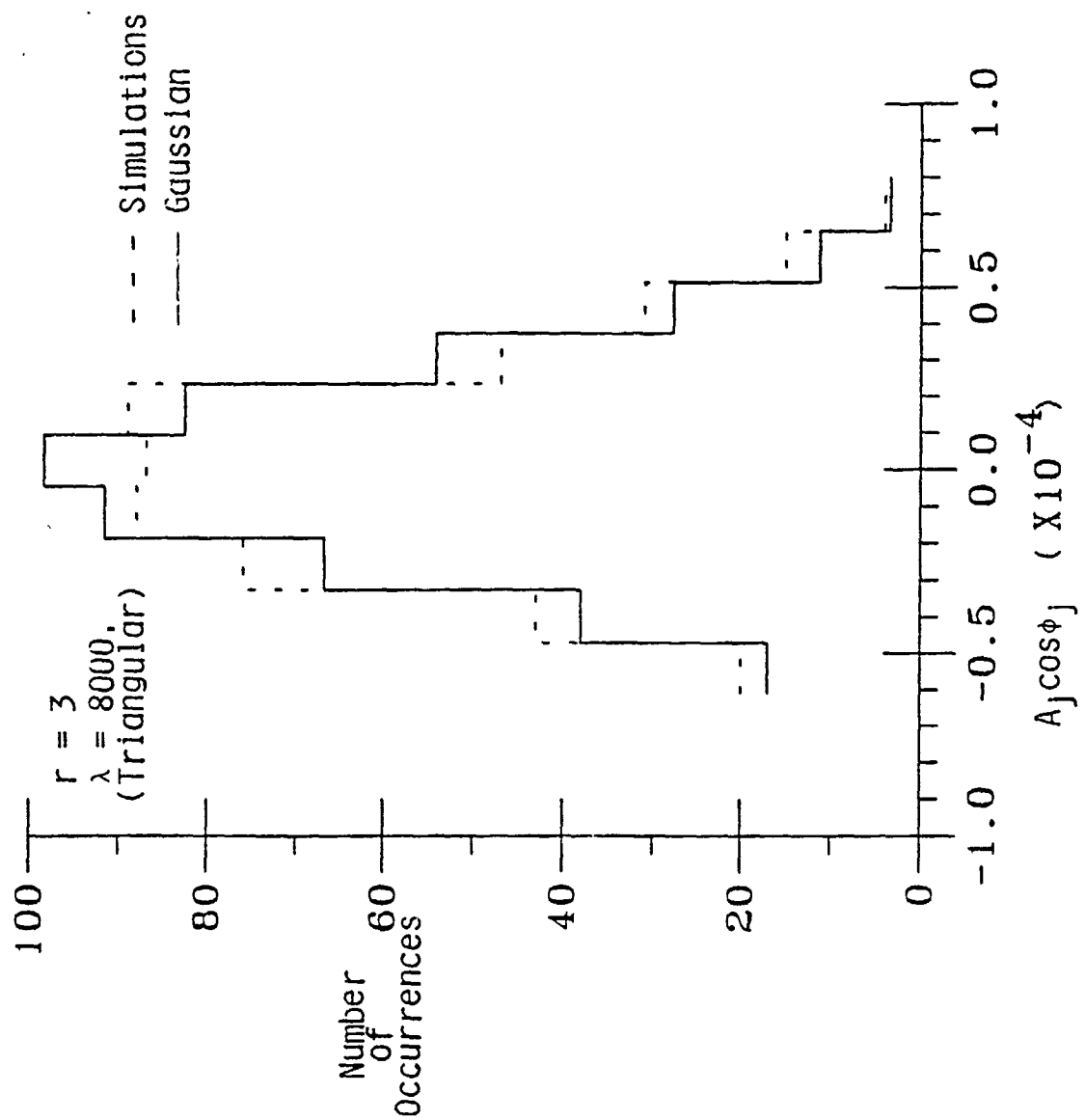


Figure 5
Senia & Chen

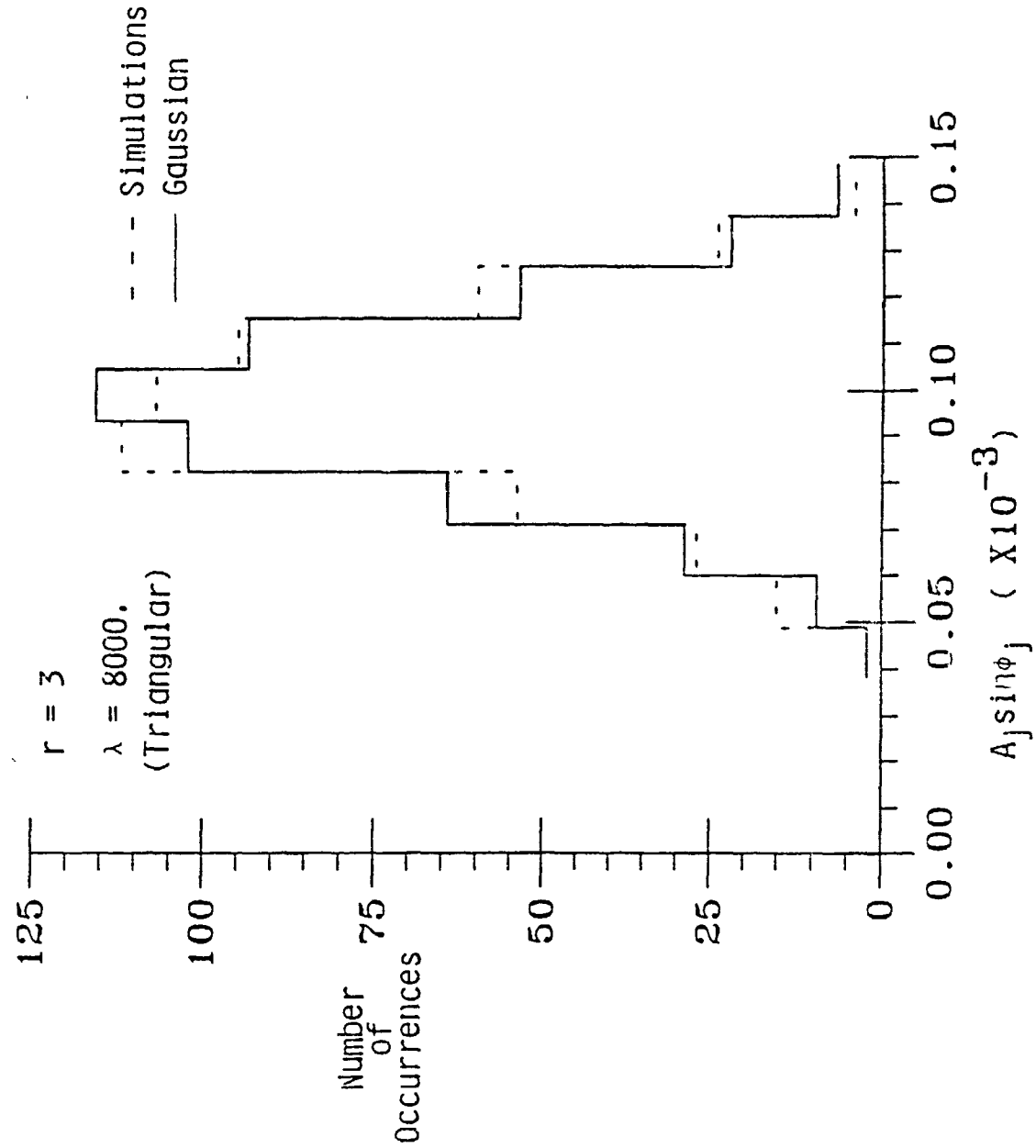
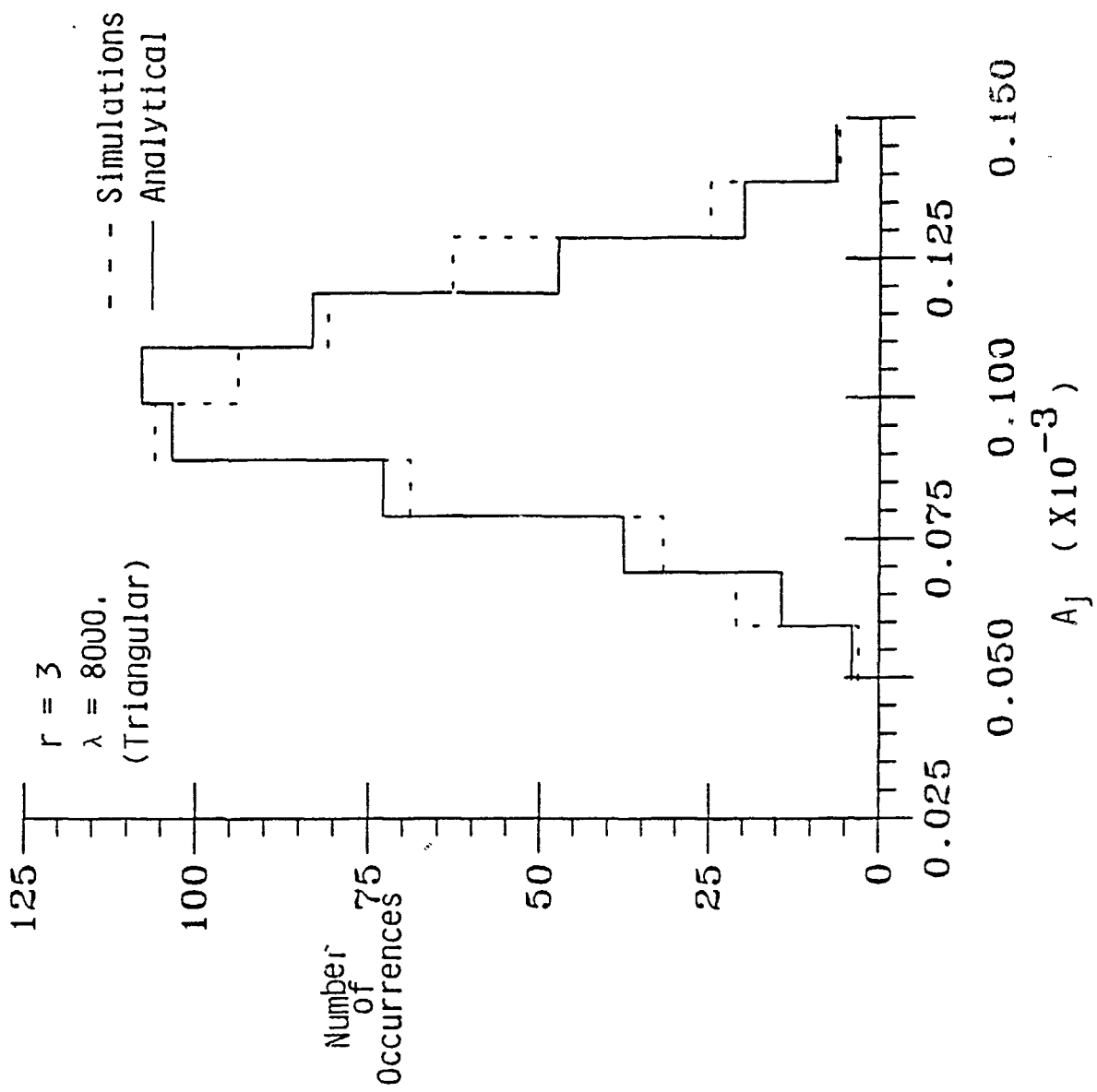


Figure 6
Sinha et al.



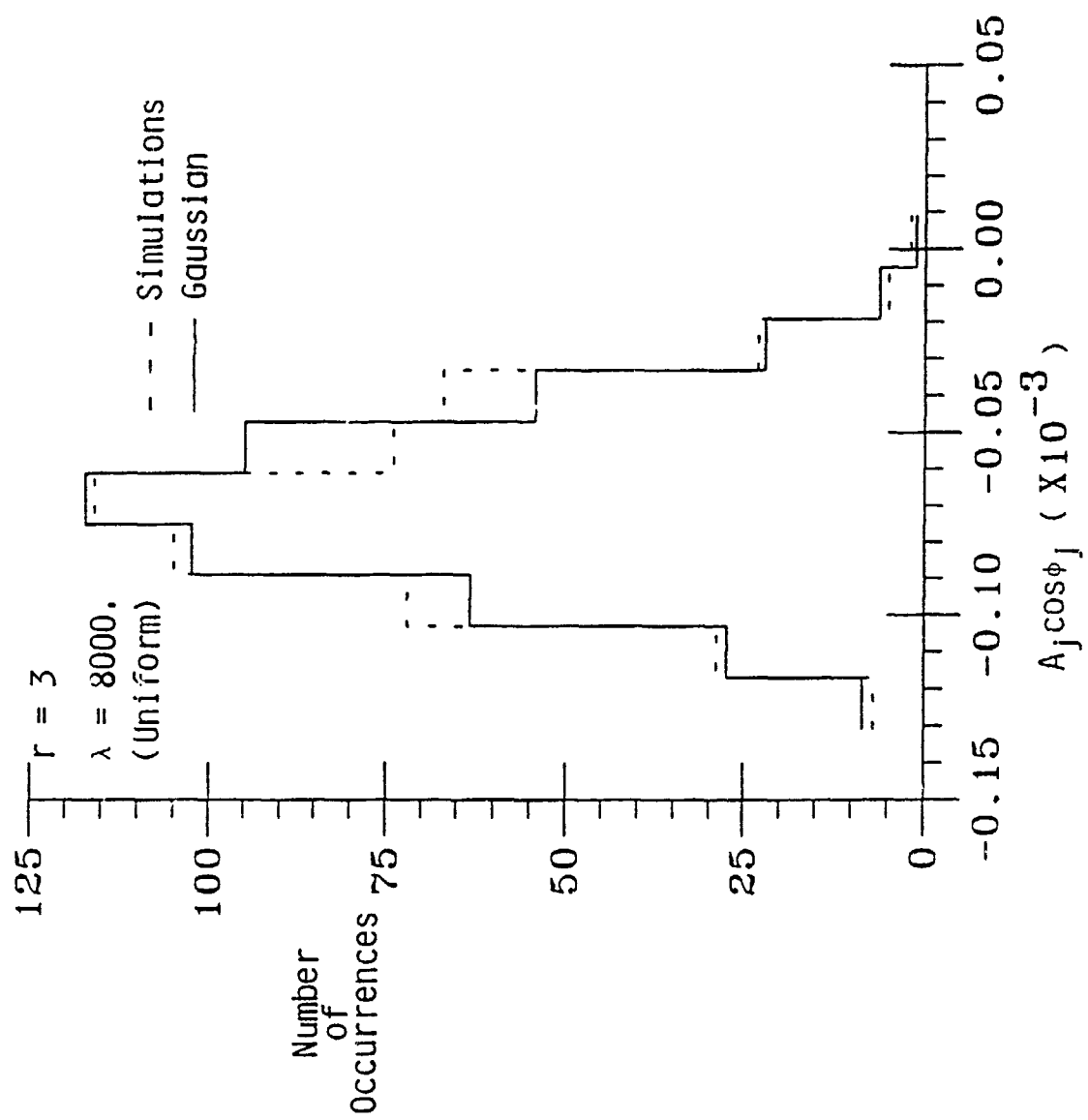


Figure 8
Saito & Chen

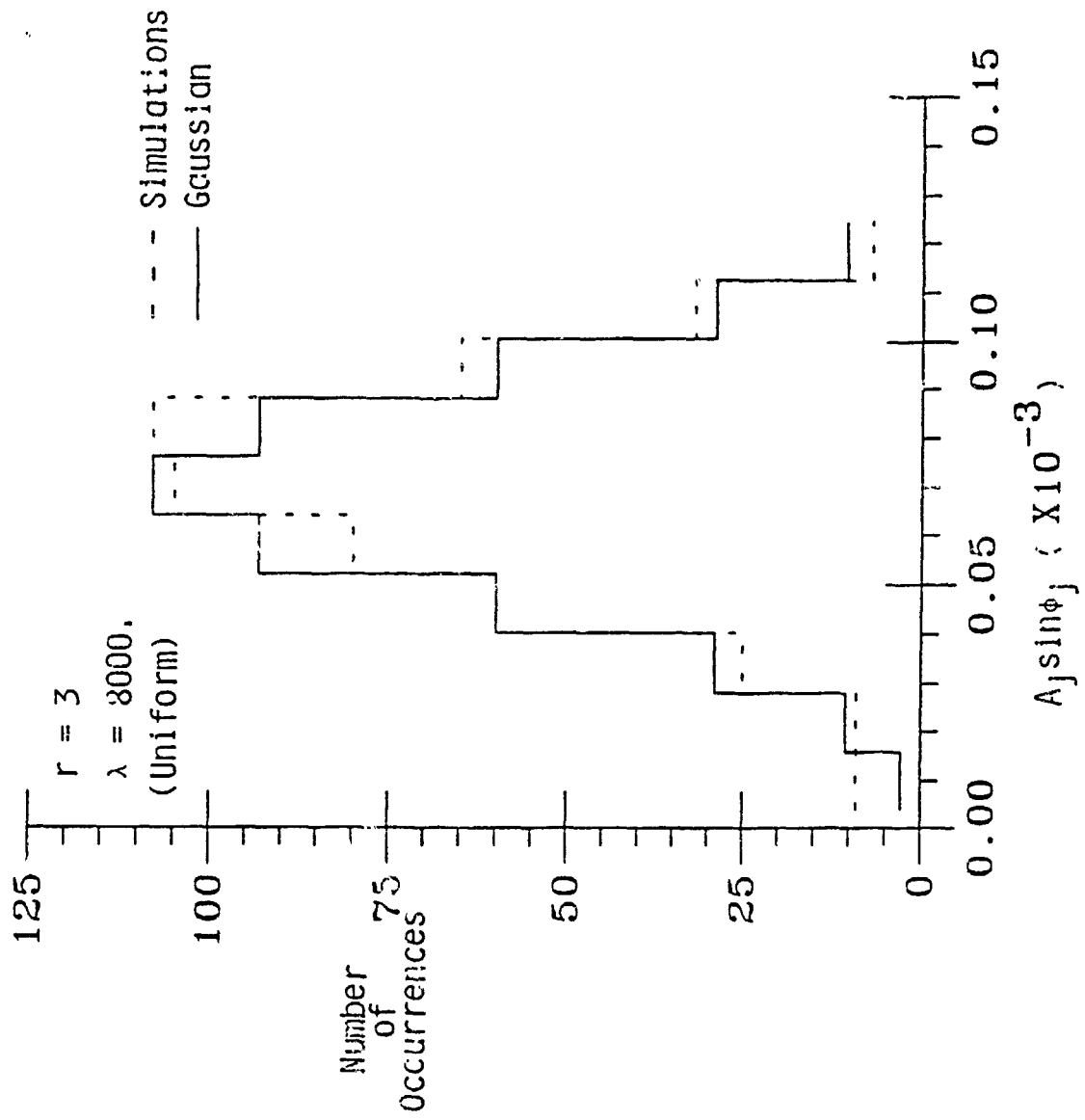
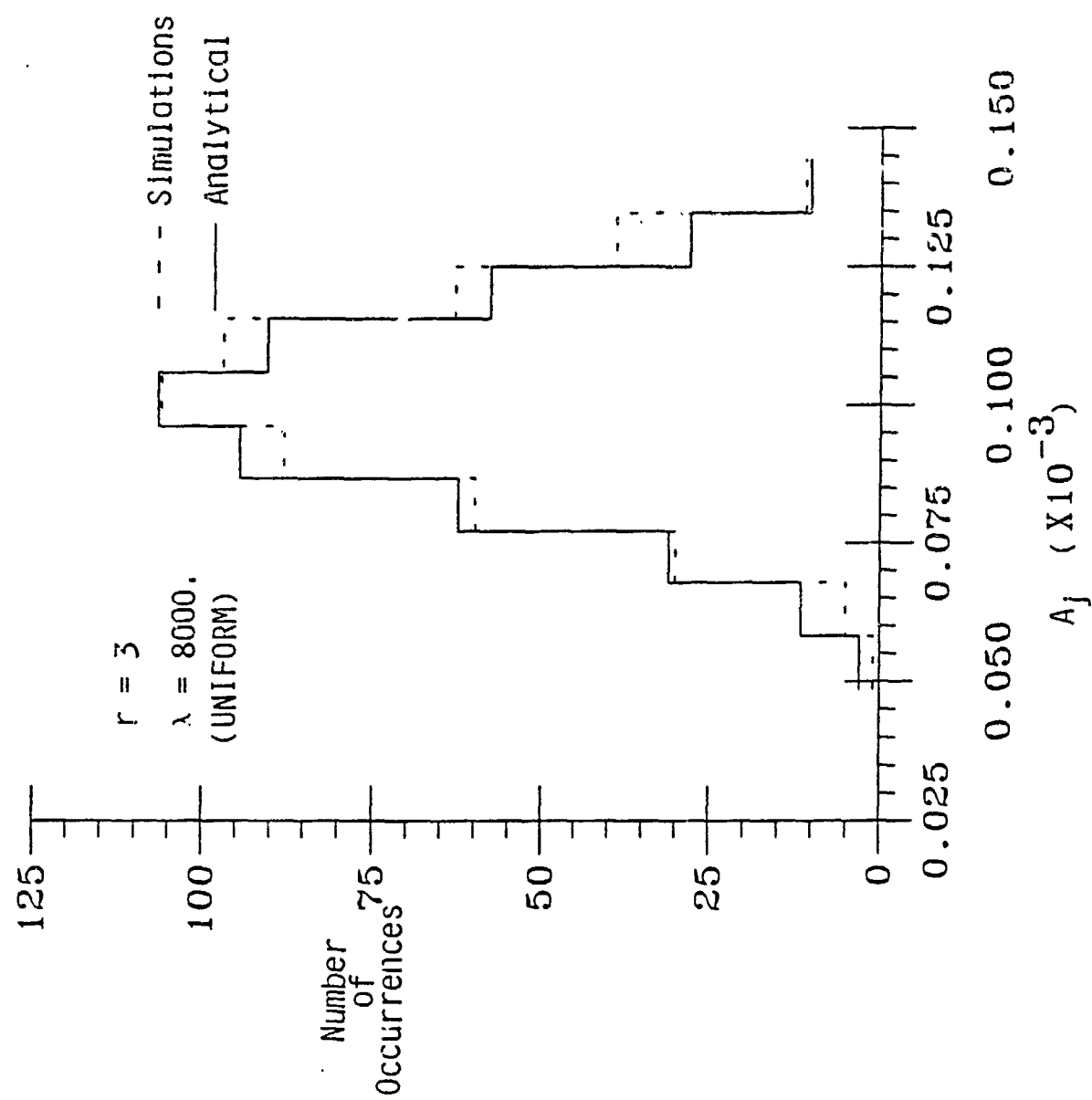
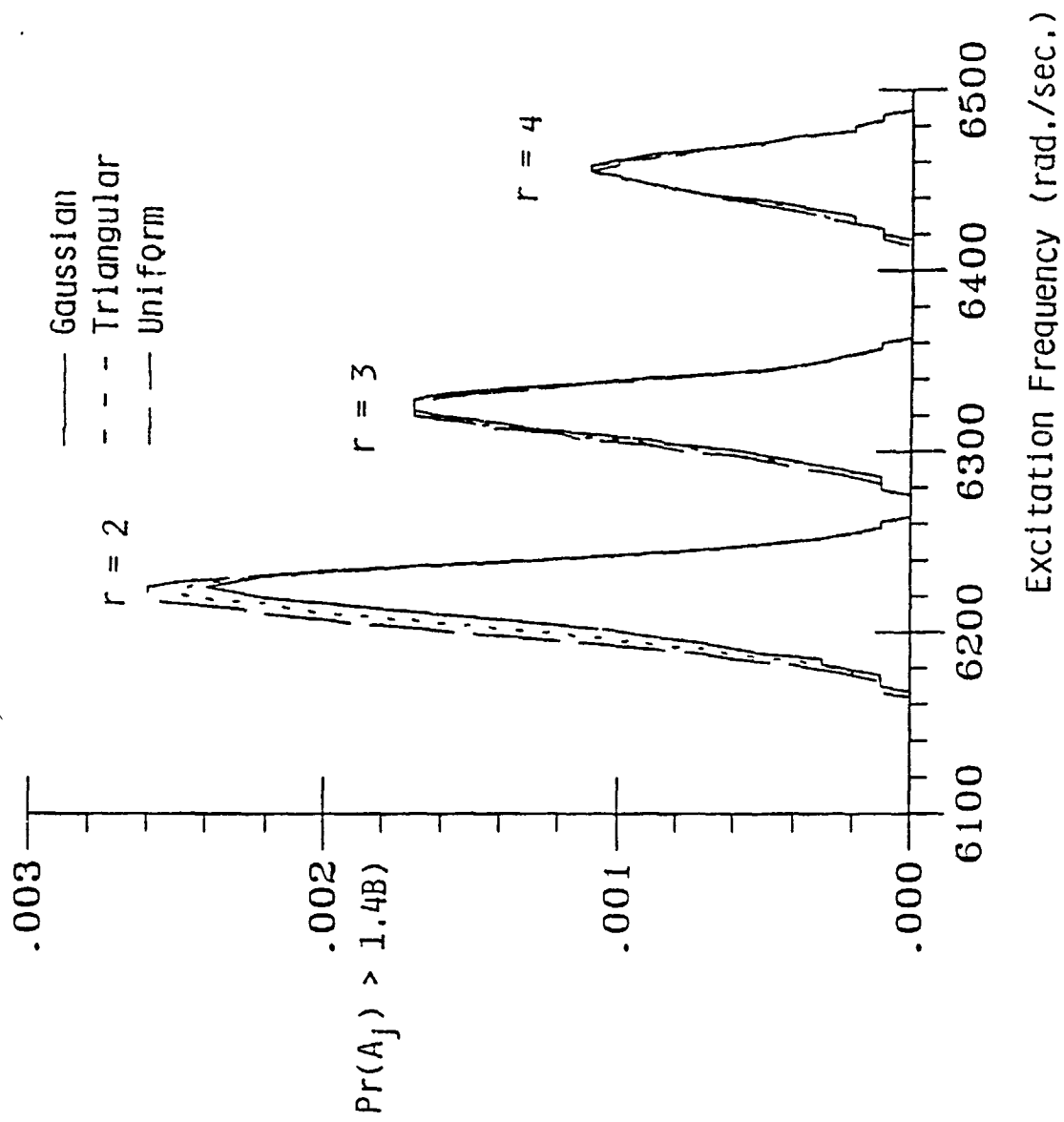
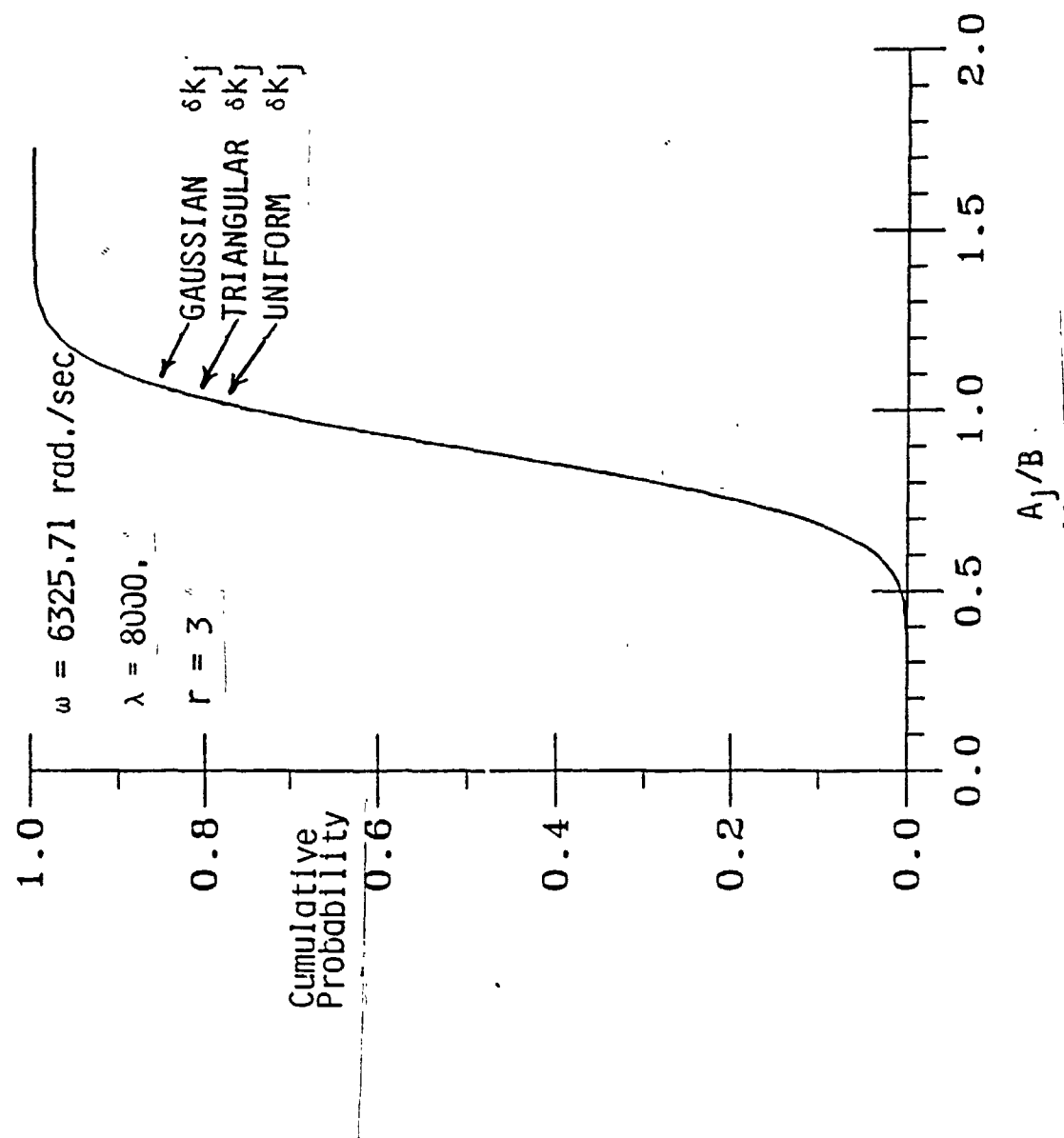


Figure 9
Srivastava & Chakraborty







SECTION 2
CALCULATING THE STATISTICS OF THE MAXIMUM AMPLITUDE
OF A MISTUNED BLADED DISK ASSEMBLY

Nomenclature

<u>Symbol</u>	<u>Meaning</u>
A_j	amplitude of x_j (mistuned system)
A_t	resonant amplitude of the tuned system
c	modal damping (tuned system)
cdf	cumulative distribution function
$\text{Cov}(y, z)$	covariance of random variables, y and z
diag	diagonal elements of a diagonal matrix
$E(y)$	expected value of random variable, y
exp	exponential
f_0	magnitude of excitation force
$f(y_1, \dots, y_n)$	joint pdf of random variables y_1, y_2, \dots, y_n
H	tuned system matrix defined in equation (9)
δH	matrix defined in equation (10)
i	$\sqrt{-1}$
I	identity matrix
k_C	structural coupling stiffness between adjacent blades
k_j	modal stiffness of j th blade (mistuned system)
k_t	modal stiffness of each blade (tuned system)
m_t	modal mass of each blade (tuned system)
$\text{Max}(A_j/A_t)$	$\text{Max}(A_1, A_2, \dots, A_N)/A_t$, maximum value
N	number of blades
pdf	probability density function
$\text{Pr}(\)$	probability
t	time
u_j	j th element of vector U

u_j'	u_j for the tuned system ($\delta k_j = 0$)
$\text{Var}(y)$	variance of random variable, y
x_j	response of j th blade (mistuned system)
β_r	interblade phase angle of r th engine order excitation
δk_j	$= k_j - k_t$
$\gamma_{y,z}$	correlation coefficient between y and z random variables
μ_y	mean of a random variable y
ω	excitation frequency (rad/sec)
ϕ_j	phase angle of x_j
ψ_j	phase angle of excitation force on the j th blade
σ_y	standard deviation of random variable y
ζ	damping ratio

1. Introduction

Mistuning in a bladed disk assembly refers to the variation in the modal properties of blades because of manufacturing tolerances. It has received a wide attention in the existing literature [1-3] because even a small amount of mistuning can lead to a large variation of blades' amplitudes within the same assembly. In fact, the amplitude of vibration of the worst blade may often be as high as one and one-half times the amplitude of a blade of a perfectly tuned system. Consequently, the fatigue life of a blade on a mistuned assembly may be significantly lower than that predicted on the basis of a perfectly tuned system. Furthermore, the deviations of the modal properties of blades from their nominal values are statistically distributed. As a result, there exists a large number of possible sets of blades' modal parameters that a bladed disk assembly can have. Since the maximum amplitude will be different for each such set of blades' modal parameters, it is important for the designer to know the statistics of the forced response, particularly the probability that the maximum amplitude on any disk would exceed a critical value in an efficient manner.

For a given distribution of modal parameters, the statistics of the blades' amplitudes can be computed by the following two approaches: 1) numerical simulations and 2) analytical technique. For numerical simulations [4,5], the modal parameters of each blade of a mistuned assembly are chosen randomly from a distribution with specified values of mean and variance. Since the steady state response of the resulting system can be easily obtained, the statistics of blades' amplitudes can be generated by considering a large number of rotor stages with different sets of blades' modal parameters. However, this approach is cumbersome and expensive in terms of computer time.

The analytical approach [6-10] yields the statistics of the forced response of a mistuned system without performing numerical simulations and, consequently, is computationally efficient. The technique developed by Huang [6] can yield the mean and the variance of a blade's amplitude. However, this analysis is valid only for rotor stages with closely spaced blades. In addition, there was no attempt to characterize the probability density function (pdf) of a

blade's amplitude. Recently, Sinha and Chen [7-10] have developed a technique to compute the statistics of the forced response of a mistuned bladed disk assembly. This technique yields the pdf of a blade's amplitude (A_j) through the joint statistics of $A_j \cos\phi_j$ and $A_j \sin\phi_j$ where ϕ_j is the phase of the j th blade. This method is valid for Gaussian and non Gaussian distributions of modal parameters as well. However, the distribution of the maximum amplitude on a bladed disk assembly was not computed.

In this paper, an alternative analytical technique is developed to directly obtain the pdf of the amplitude of a blade's vibration without using the joint statistics of $A_j \cos\phi_j$ and $A_j \sin\phi_j$. The amplitude of each blade is expanded as a Taylor's series in terms of the deviations of the modal parameters. Then, it is shown using the central limit theorem that the distribution of each amplitude is Gaussian irrespective of the nature of modal parameter distributions. On the basis of this result, an efficient technique has been developed to compute the distribution of the maximum amplitude on a bladed disk assembly. The comparison with the results from numerical simulations indicates that the analytical technique is accurate.

First, the development of the analytical technique is presented. The model for the bladed disk assembly is shown in Figure 1 and is exactly the same as used in previous papers [7-10]. Next, the results of the analytical technique are compared with those from numerical simulations.

2. Governing Equation and Steady State Response

In the model of the bladed disk assembly (Figure 1), the vibration each blade is represented by a single mode. m_j and k_j are the modal mass and stiffness, respectively. The mechanical coupling between adjacent blades due to the disk flexibility is represented by a spring with stiffness k_C . The viscous damping coefficient c is associated with each blade to represent the energy dissipation from structural and aerodynamic sources.

The mistuning of each blade is modeled by the deviation in the blade's stiffness alone. The external force on each blade is assumed to represent a particular engine order and, as a result,

is sinusoidal in time and differs in phase by a constant amount from blade to blade [11]. Under the r^{th} engine order excitation, the differential equation of motion for the j^{th} blade can be described as

$$m_j \ddot{x}_j + c \dot{x}_j + k_j x_j + kC(x_j - x_{j-1}) + kC(x_j - x_{j+1}) = f_0 \cos(\omega t + \psi_j) \quad (1)$$

where $\psi_j = (j-1)\beta_r$, $\beta_r = 2\pi/N$. Because of the periodicity of the rotor stage shown in Figure 1, $(j-1)$ is taken to be N if $j=1$, and $(j+1)$ is taken to be 1 if $j=N$. Note that $k_j = k_t + \delta k_j$ where δk_j is a random variable with zero mean. Also, the distribution of δk_p is independent of δk_i ($i \neq p$). There is no assumption made on the nature of the distributions of δk_j .

The steady state response of the mistuned system under sinusoidal excitation can be described by the harmonic motion x_j :

$$x_j = A_j \cos(\omega t + \phi_j) \quad (2)$$

Substituting (2) into (1) and then equating the coefficients of $\cos\omega t$ and $\sin\omega t$ on both sides, a system of $2N$ algebraic equations can be obtained as follows:

$$(h_1 + \delta k_j)A_j \cos \phi_j + h_3 A_j \sin \phi_j - h_2(A_{j+1} \cos \phi_{j+1} + A_{j-1} \cos \phi_{j-1}) = f_0 \cos \psi_j \quad (3)$$

$$(h_1 + \delta k_j)A_j \sin \phi_j - h_3 A_j \cos \phi_j - h_2(A_{j+1} \sin \phi_{j+1} + A_{j-1} \sin \phi_{j-1}) = f_0 \sin \psi_j \quad (4)$$

where

$$h_1 = k_t + 2kC - m_j \omega^2, \quad h_2 = kC, \quad h_3 = -c\omega \quad (5)$$

Rewriting (3) and (4) in matrix form,

$$[H + \delta H]U = F_a \quad (6)$$

where

$$U = (A_1 \cos \phi_1, A_1 \sin \phi_1, \dots, A_N \cos \phi_N, A_N \sin \phi_N)^T \quad (7)$$

$$F_a = f_0 (\cos \psi_1, \sin \psi_1, \dots, \cos \psi_N, \sin \psi_N)^T \quad (8)$$

$$H = \begin{pmatrix} h_1 & h_3 & -h_2 & 0 & 0 & 0 & \dots & -h_2 & 0 \\ -h_3 & h_1 & 0 & -h_2 & 0 & 0 & \dots & 0 & -h_2 \\ -h_2 & 0 & h_1 & h_3 & -h_2 & 0 & \dots & 0 & 0 \\ 0 & -h_2 & -h_3 & h_1 & 0 & -h_2 & \dots & 0 & 0 \\ \vdots & \vdots & \vdots & \vdots & \vdots & \vdots & \dots & \vdots & \vdots \\ -h_2 & 0 & 0 & 0 & 0 & 0 & \dots & h_1 & h_3 \\ 0 & -h_2 & 0 & 0 & 0 & 0 & \dots & -h_3 & h_1 \end{pmatrix} \quad (9)$$

The matrix H corresponds to the tuned system and is circular in nature [7]. The matrix δH contains the deviations in the modal stiffness due to mistuning and is defined as follows:

$$\delta H = \text{diag}(\delta k_r, \delta k_1, \delta k_2, \dots, \delta k_N, \delta k_N) \quad (10)$$

3. Development of the Analytical Technique

3.1 Computation of μ_{A_j} , σ_{A_j} , γ_{Ap} , A_q , and the cdf of A_j

The amplitude of a blade is expressed as a perturbation from the tuned system ($k_j=k_1$, $A_j=A_1$) case via Taylor series. Truncating the fourth and higher order terms:

$$A_j = A_1 + \sum_{i=1}^N \frac{\partial A_j}{\partial k_i} \delta k_i + \frac{1}{2!} \sum_{i=1}^N \sum_{j=1}^N \frac{\partial^2 A_j}{\partial k_i \partial k_j} \delta k_i \delta k_j + \frac{1}{3!} \sum_{i=1}^N \sum_{j=1}^N \sum_{m=1}^N \frac{\partial^3 A_j}{\partial k_i \partial k_j \partial k_m} \delta k_i \delta k_j \delta k_m \quad (11)$$

where $\delta k_j = k_j - k_1$

For any give model, partial derivatives $\left(\frac{\partial A_j}{\partial k_i}, \frac{\partial^2 A_j}{\partial k_i \partial k_j} \text{ and } \frac{\partial^3 A_j}{\partial k_i \partial k_j \partial k_m} \text{ etc.} \right)$ can be computed in a recursive manner (Appendix A). Having obtained these partial derivatives, the mean (μ_{A_j}), the variance (σ_{A_j}), and correlation coefficient between A_p and A_q (γ_{Ap}, A_q) can be directly computed (Appendix B). From equation (11), A_j is a combination of a large number of random variables which are not highly dependent [8]. Therefore, the distribution of A_j can be

approximated as Gaussian for a large number of blades (N) by the central limit theorem [12]; i.e.

$$f(A_j) = \frac{1}{\sigma_{A_j} \sqrt{2\pi}} \exp^{-\frac{(A_j - \mu_{A_j})^2}{2\sigma^2_{A_j}}} \quad (12)$$

Any linear combination of amplitudes; i.e., $\sum_{j=1}^N \alpha_j A_j$ where α_j are arbitrary numbers,

will also be a combination of a large number of random variables which are not highly dependent. Consequently, it can also be approximated to be Gaussian. This implies [13] that the joint distributions $f(A_1, A_2, \dots, A_N)$ of amplitudes is Gaussian; i.e.

$$f(A_1, A_2, \dots, A_N) = \frac{1}{\sqrt{(2\pi)^N |\eta|}} \exp^{-\frac{1}{2} \eta^{-1} B^T \eta} \quad (13)$$

where $\mathbf{A} = [A_1, A_2, \dots, A_N]$

$$\mathbf{B} = \mathbf{A} - E(\mathbf{A})$$

$$(\eta)_{ij} = E(A_i A_j) - E(A_i) E(A_j)$$

$$|\eta| = \det \eta$$

Furthermore, it should be noted that the distributions of $A_j \cos \phi_j$ and $A_j \sin \phi_j$ have also been found to be Gaussian [8]; and A_j depends on $A_j \cos \phi_j$ and $A_j \sin \phi_j$ in a nonlinear fashion as follows:

$$A_j = \left(A_j^2 \cos^2 \phi_j + A_j^2 \sin^2 \phi_j \right)^{1/2} \quad (14)$$

However, it has been found that $E(A_j)$ and $E(A_j^2)$ can be predicted with a good accuracy by linearizing equation (14) around the tuned system response; i.e.,

$$\begin{aligned} A_j \approx A_t + \frac{1}{2} A_t^{-1/2} & (A_j \cos \phi_j - u_{2j-1}^t) \\ & + \frac{1}{2} A_t^{-1/2} (A_j \sin \phi_j - u_{2j}^t) \end{aligned} \quad (15)$$

The expression (15) indicates that A_j can be approximated as a linear combination of $A_j \cos \phi_j$ and $A_j \sin \phi_j$ for the typical level of mistuning. Hence, the result that the distributions of A_j , $A_j \cos \phi_j$ and $A_j \sin \phi_j$ are Gaussian can be explained.

3.2 Distribution of the Maximum Amplitude

Since the failure of a rotor stage often results from one broken blade which corresponds to the maximum amplitude, the most important information for the designer is to know the statistics of the maximum amplitude on a disk. The cdf of the maximum amplitude among the given N blades' amplitudes (A_j) on a disk can be expressed as follows

$$\begin{aligned} \Pr(\text{Max}(A_1, A_2, \dots, A_N) \leq M_A) \\ = \Pr(A_1 \leq M_A, A_2 \leq M_A, \dots, A_N \leq M_A) \\ = \int_0^{M_A} \int_0^{M_A} \dots \int_0^{M_A} f(A_1, A_2, \dots, A_N) dA_1 dA_2 \dots dA_N, \end{aligned} \quad (16)$$

where M_A is a constant.

As discussed in section 3.1, the joint pdf $f(A_1, A_2, \dots, A_N)$ can be approximated to be jointly Gaussian. Since $E(A_j)$ and the covariance matrix η can be analytically computed (Appendix B), one can theoretically evaluate the integral in equation (16). However, in practice, the number of blades on a disk is often large, e.g. $N = 56$ [11], $N = 72$ [4-5]. Therefore, a hyper-dimensional integration like equation (16) for a general function $f(A_1, A_2, \dots, A_N)$ will become extremely expensive or may be impossible in terms of the computational cost. Hence, in order to efficiently evaluate the integral in (16), further assumptions are imposed on the pdf, $f(A_1, A_2, \dots, A_N)$.

If the effects of the off-diagonal terms of the covariance matrix, η , can be neglected, the N -dimensional integration (16) can be reduced to N one-dimensional integrals as follows

$$\Pr(\text{Max}(A_1, A_2, \dots, A_N) \leq M_A) = \prod_{j=1}^N \int_0^{M_A} f(A_j) dA_j, \quad (17)$$

Furthermore, the pdf of each A_j is identical as each k_j has an identical distribution [14]. Therefore, equation (17) can be further simplified as follows

$$\Pr(\text{Max}(A_1, A_2, \dots, A_N) \leq M_A) = \left(\int_0^{M_A} f(A_1) dA_1 \right)^N \quad (18)$$

Comparing equations (16) and (18), it can be seen that an almost impossible N -dimensional integration has been reduced to a simple one-dimensional integration. The validity

of equation (18) is established in the next section. It should be noted that the distribution of the maximum amplitude is not Gaussian.

4. Comparison with Numerical Simulations

In order to verify the accuracy of the analytical technique, the analytical results are compared with those from numerical simulations. For numerical simulations, the steady state responses, $A_j \cos \phi_j$ and $A_j \sin \phi_j$, of the mistuned bladed disk assemblies are obtained by solving the $2N$ simultaneous linear equations (3) and (4). Then, the statistics of A_j and $\text{Max}(A_j)$ are computed from a large sample (arbitrarily chosen to be 3000) of bladed disk assemblies with different sets of deviations in blades' modal parameters, δk_j . The values of δk_j are chosen from a Gaussian¹ distribution with specified means and variances. The IMSL [15] subroutine DRNNOA, has been used to generate the Gaussian distributions.

The number of blades is chosen to be twenty-four. The excitation frequency is chosen to be 6328.8 rad/sec, which corresponds to the resonant condition for the tuned system under the third engine order excitation ($r=3$). The third engine order corresponds to the 45 degree interblade phase angle of the excitation forces. The nominal values of system parameters are shown in Table 1 and they are representative of a high pressure turbine stage [4]. The damping value, $c = 1.443$ Newton-sec/meter, corresponds to about 1.0% damping factor, which is typical of those observed in gas turbine engine rotor stages from aerodynamic and structural sources [5].

In order to test the accuracy of the analytical results, the standard deviations ($\sigma_{\delta k_j}$) of the mistuned stiffnesses are chosen to be 7500 Newton/meter and 10000 Newton/meter, respectively. Also, $E(\delta k_j) = 0$.

¹ The distributions of amplitudes have been found to be insensitive to the types of modal parameters' distributions [9].

4.1 Distribution of Amplitudes

From Figure 2, it can be seen that the analytical results compare well with those from the numerical simulation, even though the accuracy of the analytical result decreases as the value of $\sigma_{\delta k_j}$ increases.

4.2 Distribution of the Maximum Amplitude

As shown in Figure 3, the distribution of the normalized maximum amplitude $\text{Max}(A_j/A_t)$ (A_t is the resonant amplitude of the tuned system) from the analytical technique, equation (18), compares well with that from the numerical simulation for $\sigma_{\delta k_j} = 7500$. However, for $\sigma_{\delta k_j} = 10000$, the accuracy becomes smaller. This is due to the error in estimating the distribution of the amplitude by the analytical technique, equation (12), for $\sigma_{\delta k_j} = 10000$. It should be noted that the analytical approximation, equation (18), is found to be quite accurate if the distribution of the amplitude from the numerical simulation is used, Figure 3(b).

The magnitudes of the off-diagonal terms in the covariance matrix, η can be evaluated by examining the correlation coefficients, $\gamma_{Ap,Aq}$. Because of the periodicity, it has been found that the values of $\gamma_{Am,Aj}$ depend on $|m-j|$. Hence, only the values of $\gamma_{A1,Aj}$ are presented here. As shown in Figure 4 for each $\sigma_{\delta k_j}$, the correlation coefficients ($\gamma_{A1,Aj}$) oscillate around zero and decrease as the distance between two blades increases. Also, the absolute values of most of $\gamma_{A1,Aj}$ are small and almost half of them are very close to zero. Even though some of $\gamma_{A1,Aj}$ are not zero, the cumulative effects of the off-diagonal terms in the covariance matrix, η , are small and the accuracy of the analytical technique, equation (18), is acceptable (Figure 3).

As mentioned earlier, the correlation coefficients, $\gamma_{A1,Aj}$, decrease from the nearer neighbours to the farther ones, Figure 4. This implies that the magnitudes of the off-diagonal terms, $\gamma_{Am,Aj}$, become smaller as $|m-j|$ becomes larger. Hence, one should expect the accuracy of the analytical results to be better for the rotor stage with a larger number of blades, while

worse for that with a smaller number of blades. To study this effect, the number of blades is chosen to be $N = 8$ and $N = 56$. The standard deviation of δk_j is equal to 7500.

As shown in Figure 5, relatively, most of the $\gamma A_1, A_j$ are not zero for $N = 8$, while for $N = 56$ more than four-fifths of the $\gamma A_1, A_j$ are close to zero. Hence, the accuracy of the distribution of the $\text{Max}(A_j/A_1)$ from the analytical technique is worse of $N = 8$, while much better for $N = 56$, Figure 6. Since the number of blades is often large in practice (e.g. $N = 56$ [11], $N = 72$ [4,5], the analytical approximation, equation (18), may be successfully applied in these practical situations.

5 Conclusions

To efficiently compute the statistics of the maximum amplitude of a mistuned bladed disk assembly, an analytical technique has been developed in this paper. The analytical technique uses the direct Taylor series expansion in terms of the perturbations in an amplitude as a function of perturbations in modal stiffnesses. This technique can compute the mean, the variance, the cdf of an amplitude, and the correlation coefficients between any two amplitudes. Also, the cdf of the maximum amplitude on a rotor stage can be computed.

The validity of the analytical technique has been corroborated by comparison with the results from the numerical simulation. Also, the analytical technique developed in this paper is valid for Gaussian and non-Gaussian mistuned parameters as well. The CPU time for the analytical technique is found to be much smaller than that for numerical simulations. On a VAX 8550 computer, the CPU time for numerical simulations and the analytical technique are 1079 seconds and 9.59 seconds, respectively for $N = 56$ and $\sigma \delta k_j = 10000$.

APPENDIX A

COMPUTATION OF $\frac{\partial A_j}{\partial k_i}$, $\frac{\partial^2 A_j}{\partial k_i \partial k_j}$ AND $\frac{\partial^3 A_j}{\partial k_i \partial k_j \partial k_m}$

From (7), the amplitude, A_j , can be represented as

$$A_j = (u_{2j-1}^2 + u_{2j}^2)^{\frac{1}{2}} \quad (A.1)$$

Continually differentiating (A.1),

$$\frac{\partial A_j}{\partial k_i} = \frac{1}{A_j} \left(u_{2j-1} \frac{\partial u_{2j-1}}{\partial k_i} + u_{2j} \frac{\partial u_{2j}}{\partial k_i} \right), \quad (A.2)$$

$$\begin{aligned} \frac{\partial^2 A_j}{\partial k_i \partial k_j} = \frac{1}{A_j} & \left(- \frac{\partial A_j}{\partial k_i} \frac{\partial A_j}{\partial k_j} + \frac{\partial u_{2j-1}}{\partial k_i} \frac{\partial u_{2j-1}}{\partial k_j} + \frac{\partial u_{2j}}{\partial k_i} \cdot \frac{\partial u_{2j}}{\partial k_j} \right. \\ & \left. + u_{2j-1} \frac{\partial^2 u_{2j-1}}{\partial k_i \partial k_j} + u_{2j} \frac{\partial^2 u_{2j}}{\partial k_i \partial k_j} \right) \end{aligned} \quad (A.3)$$

and for $p > 2$,

$$\begin{aligned} \frac{\partial^p A_j}{\partial s_1 \partial s_2 \dots \partial s_p} = \frac{1}{A_j} & \left[\left(\sum_{i=1}^3 \sum_{q=1}^p \text{sign}(g_i) \frac{\partial g_i}{\partial s_q} \frac{\partial^{p-1} g_i}{\partial s_1 \dots \partial s_{q-1} \partial s_{q+1} \dots \partial s_p} \right) \right. \\ & \left. + u_{2j-1} \frac{\partial^p u_{2j-1}}{\partial s_1 \partial s_2 \dots \partial s_p} + u_{2j} \frac{\partial^p u_{2j}}{\partial s_1 \partial s_2 \dots \partial s_p} \right] \end{aligned} \quad (A.4)$$

where s_1, s_2, \dots, s_p represent a combination of p variables chosen from N variables, k_j . And,

$g_1 = A_j, g_2 = u_{2j-1}, g_3 = u_{2j}, \text{sign}(g_1) = -1, \text{sign}(g_2) = \text{sign}(g_3) = 1$. From equation (6),

$$\frac{\partial U}{\partial s_1 \partial s_2 \dots \partial s_p} = - (H + \delta H)^{-1} \sum_{q=1}^p \frac{\partial (H + \delta H)}{\partial s_q} \frac{\partial^{p-1} U}{\partial s_1 \dots \partial s_{q-1} \partial s_{q+1} \dots \partial s_p}, \quad (A.5)$$

where $\partial(H + \delta H)/\partial s_q$ can be obtained for a given model of the bladed disk assembly. For the

model shown in Figure 1,

$$\frac{\partial (H + \delta H)}{\partial s_q} = \text{diag} [0 \dots \frac{1}{2j-1} \frac{1}{2j} \dots 0] \quad (A.6)$$

where $s_q = k_j$. If $(H^{-1})_{p,q} = a_{p,q}$,

$$\frac{\partial u_{2m-1}}{\partial k_j} = -u_{2j-1}a_{2m-1,2j-1} - u_{2j}a_{2m-1,2j} \quad (A.7)$$

$$\frac{\partial u_{2m}}{\partial k_j} = -u_{2j-1}a_{2m,2j-1} - u_{2j}a_{2m,2j} \quad (A.8)$$

$$\begin{aligned} \frac{\partial^2 u_{2m-1}}{\partial k_j \partial k_\ell} = & - \left(a_{2m-1,2\ell-1} \frac{\partial u_{2\ell-1}}{\partial k_j} + a_{2m-1,2\ell} \frac{\partial u_{2\ell}}{\partial k_j} \right. \\ & \left. + a_{2m-1,2j-1} \frac{\partial u_{2j-1}}{\partial k_\ell} + a_{2m-1,2j} \frac{\partial u_{2j}}{\partial k_\ell} \right), \end{aligned} \quad (A.9)$$

$$\frac{\partial^2 u_{2m}}{\partial k_j \partial k_\ell} = - \left(a_{2m,2\ell-1} \frac{\partial u_{2\ell-1}}{\partial k_j} + a_{2m,2\ell} \frac{\partial u_{2\ell}}{\partial k_j} + a_{2m,2j-1} \frac{\partial u_{2j-1}}{\partial k_\ell} + a_{2m,2j} \frac{\partial u_{2j}}{\partial k_\ell} \right) \quad (A.10)$$

$$\begin{aligned} \frac{\partial^3 u_{2m-1}}{\partial k_\ell \partial k_j \partial k_i} = & - \left(a_{2m-1,2i-1} \frac{\partial^2 u_{2i-1}}{\partial k_\ell \partial k_j} + a_{2m-1,2i} \frac{\partial^2 u_{2i}}{\partial k_\ell \partial k_j} + a_{2m-1,2j-1} \frac{\partial^2 u_{2j-1}}{\partial k_\ell \partial k_i} \right. \\ & \left. + a_{2m-1,2j} \frac{\partial^2 u_{2j}}{\partial k_\ell \partial k_i} + a_{2m-1,2\ell-1} \frac{\partial^2 u_{2\ell-1}}{\partial k_j \partial k_i} + a_{2m-1,2\ell} \frac{\partial^2 u_{2\ell}}{\partial k_j \partial k_i} \right) \end{aligned} \quad (A.11)$$

$$\begin{aligned} \frac{\partial^3 u_{2m}}{\partial k_\ell \partial k_j \partial k_i} = & - \left(a_{2m,2i-1} \frac{\partial^2 u_{2i-1}}{\partial k_\ell \partial k_j} + a_{2m,2i} \frac{\partial^2 u_{2i}}{\partial k_\ell \partial k_j} + a_{2m,2j-1} \frac{\partial^2 u_{2j-1}}{\partial k_\ell \partial k_i} \right. \\ & \left. + a_{2m,2j} \frac{\partial^2 u_{2j}}{\partial k_\ell \partial k_i} + a_{2m,2\ell-1} \frac{\partial^2 u_{2\ell-1}}{\partial k_j \partial k_i} + a_{2m,2\ell} \frac{\partial^2 u_{2\ell}}{\partial k_j \partial k_i} \right) \end{aligned} \quad (A.12)$$

It should be noted that all the partial derivatives are evaluated at the tuned system ($k_j = k_t$) response. Furthermore, since

$$\frac{\partial^2 A_j}{\partial k_i \partial k_\ell} = \frac{\partial^2 A_j}{\partial k_\ell \partial k_i}, \quad (A.13)$$

and

$$\begin{aligned} \frac{\partial^3 A_j}{\partial k_i \partial k_\ell \partial k_m} &= \frac{\partial^3 A_j}{\partial k_i \partial k_m \partial k_\ell} = \frac{\partial^3 A_j}{\partial k_\ell \partial k_i \partial k_m} \\ &= \frac{\partial^3 A_j}{\partial k_\ell \partial k_m \partial k_i} = \frac{\partial^3 A_j}{\partial k_m \partial k_i \partial k_\ell} = \frac{\partial^3 A_j}{\partial k_m \partial k_\ell \partial k_i}, \end{aligned} \quad (A.14)$$

only one term has to be computed in the above two groups, (A.13) and (A.14).

APPENDIX B
CALCULATION OF μ_{A_j} , $\sigma_{A_j}^2$ AND γ_{A_j, A_i}

From equation (11),

$$A_p = A_t + \sum_{i=1}^N \frac{\partial A_p}{\partial k_i} \delta k_i + \frac{1}{2!} \sum_{i=1}^N \sum_{j=1}^N \frac{\partial^2 A_p}{\partial k_i \partial k_j} \delta k_i \delta k_j + \frac{1}{3!} \sum_{i=1}^N \sum_{j=1}^N \sum_{k=1}^N \frac{\partial^3 A_p}{\partial k_i \partial k_j \partial k_k} \delta k_i \delta k_j \delta k_k. \quad (21)$$

Then the above equation can be expressed as

$$A_p - A_t = t_p + w_p + y_p, \quad (B.1)$$

where

$$t_p = \sum_{j=1}^N t_{p,j} (\delta k_j) \quad t_{p,j} = \frac{\partial A_p}{\partial k_j}, \quad (B.2)$$

$$w_p = \sum_{j=1}^N \sum_{k=1}^N w_{p,j,k} (\delta k_j) (\delta k_k) \quad w_{p,j,k} = \frac{1}{2!} \frac{\partial^2 A_p}{\partial k_j \partial k_k}, \quad (B.3)$$

$$y_p = \sum_{j=1}^N \sum_{k=1}^N \sum_{l=1}^N y_{p,j,k,l} (\delta k_j) (\delta k_k) (\delta k_l) \quad y_{p,j,k,l} = \frac{1}{3!} \frac{\partial^3 A_p}{\partial k_j \partial k_k \partial k_l}. \quad (B.4)$$

Then μ_{A_j} , $\sigma_{A_j}^2$ and γ_{A_j, A_i} can be computed from Ref. [8].

References

1. Ewins, D.J. and Srinivasan, A.V. (Editors), Vibration of Bladed Disk Assemblies, ASME, 1983.
2. Kielb, R.E. and Reiger, N.F. (Editors), Vibration of Blades and Bladed Disk Assemblies, ASME, 1985.
3. Kielb, R.D., Crawley, E. and Simonis, J.C. (Editors), Bladed Disk Assemblies, ASME DE-Vol. 6, 1987
4. Griffin, J.H. and Hoosac, T.M., "Model Development and Statistical Investigation of Turbine Blade Mistuning," Journal of Vibration, Acoustics, Stress and Reliability in Design, Vol. 106, April 1984, pp. 204-210.
5. Basu, P. and Griffin, J.H., "The Effect of Limiting Aerodynamic and Structural Coupling in Models of Mistuned Bladed Disk Vibration," Journal of Vibration, Acoustics, Stress, and Reliability in Design, Vol. 108, April 1986, pp. 132-139.
6. Huang, Wen-Hu, "Vibration of Some Structures with Periodic Random Parameters," AIAA Journal, Vol. 20, No. 7, 1982, pp. 1001-1008.
7. Sinha, A., "Calculating the Statistics of Forced Response of a Mistuned Bladed Disk Assembly," AIAA Journal Vol. 24, No. 11, 1986, pp. 1797-1801.
8. Sinha, A. and Chen, S., "A Higher-Order Technique to Calculate the Statistics of Forced Response of a Mistuned Bladed Disk Assembly," Journal of Sound and Vibration, April 1989.
9. Sinha, A. and Chen, S., "Probabilistic Analysis of Forced Response of a Mistuned Bladed Disk Assembly with Various Mistuning Distributions," AIAA paper #88-2399, Proceedings of the 29th AIAA/ASME/ASCE/AHS Structures, Structural Dynamics and Materials Conference, April 1988, pp. 1487-1494.
10. Chen, S. and Sinha, A., "Calculating the Statistics of Forced Response of a Mistuned Bladed Disk Assembly with Friction Dampers," Submitted to ASME Journal of Vibration, Acoustics, Stress and Reliability in Design.
11. Kaza, K.R.V. and Kielb, R.E., "Flutter and Response of Mistuned Cascade in Incompressible Flow," AIAA Journal, Vol. 20, No. 8, August 1982, pp. 1120-1127.
12. Benjamin, J.R. and Cornell, C.A., "Probability, Statistics and Decision for Civil Engineers," McGraw-Hill Co., 1970, pp. 251-253.
13. Papoulis, A., "Probability, Random Variables and Stochastic Processes," McGraw-Hill Co., 1965.
14. Chen, S., "Efficient Computation of the Statistics of Forced Response of a Mistuned Bladed Disk Assembly with Friction Dampers," Ph.D. Thesis, Department of Mechanical Engineering, PSU, University Park, PA, 1989.

15. IMSL Reference Manual, Houston, TX, 1987.

Table 1 Data for Simulation (SI Unit)

$m_t = 0.0114$ $kC = 45430.0$

$k_t = 430000.0$ $c = 1.443$

$f_0 = 1.0$

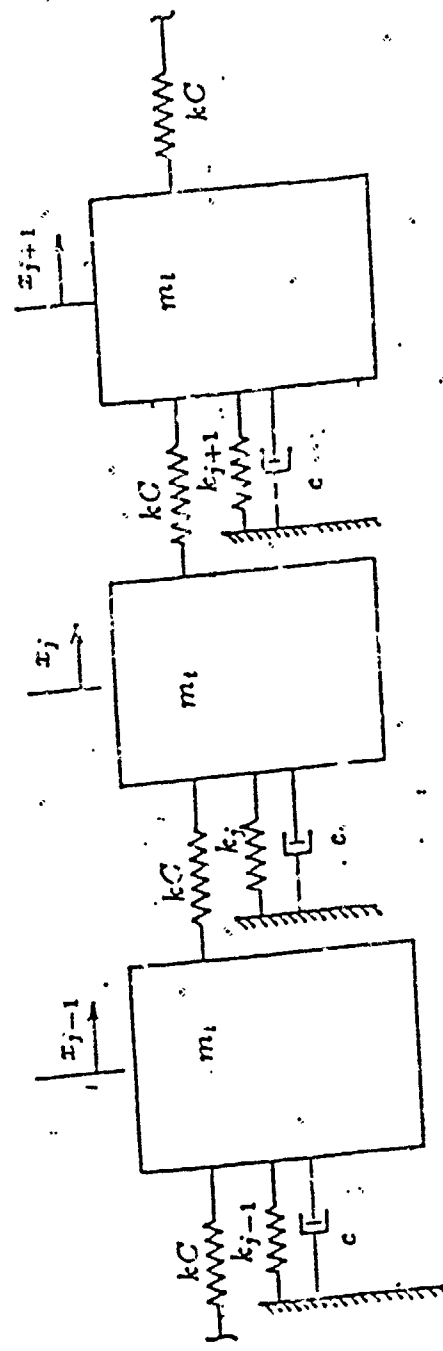


Figure 1. Spring/Mass Model of a Rotor Stage (Linear System)

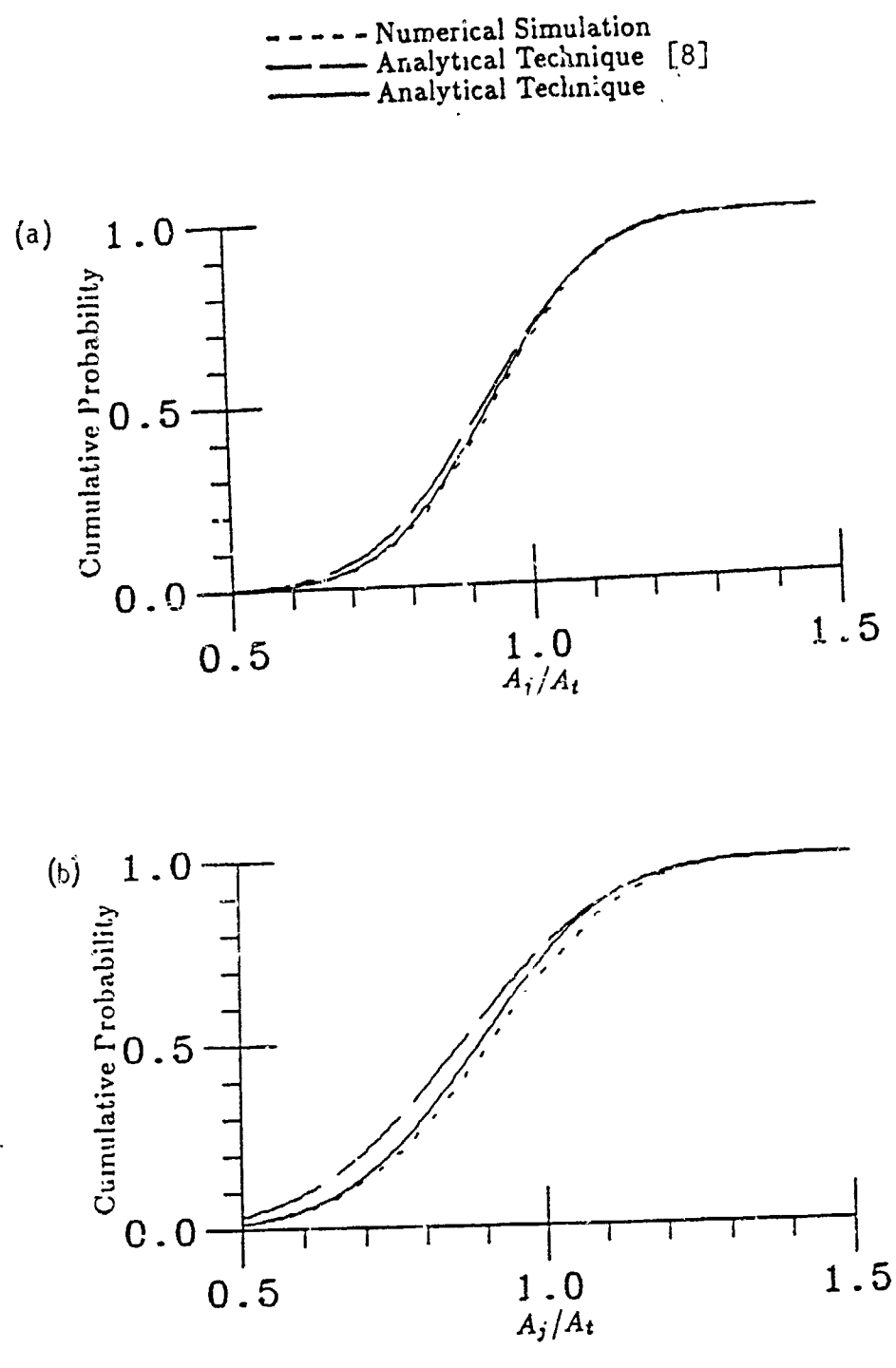


Figure 2 cdf of A_j : Numerical Simulation and Analytical Technique $N = 24$, $c = 1.443$, $\beta_r = 45^\circ$, (a) $\sigma_{dkj} = 7500$ (b) $\sigma_{dkj} = 10000$

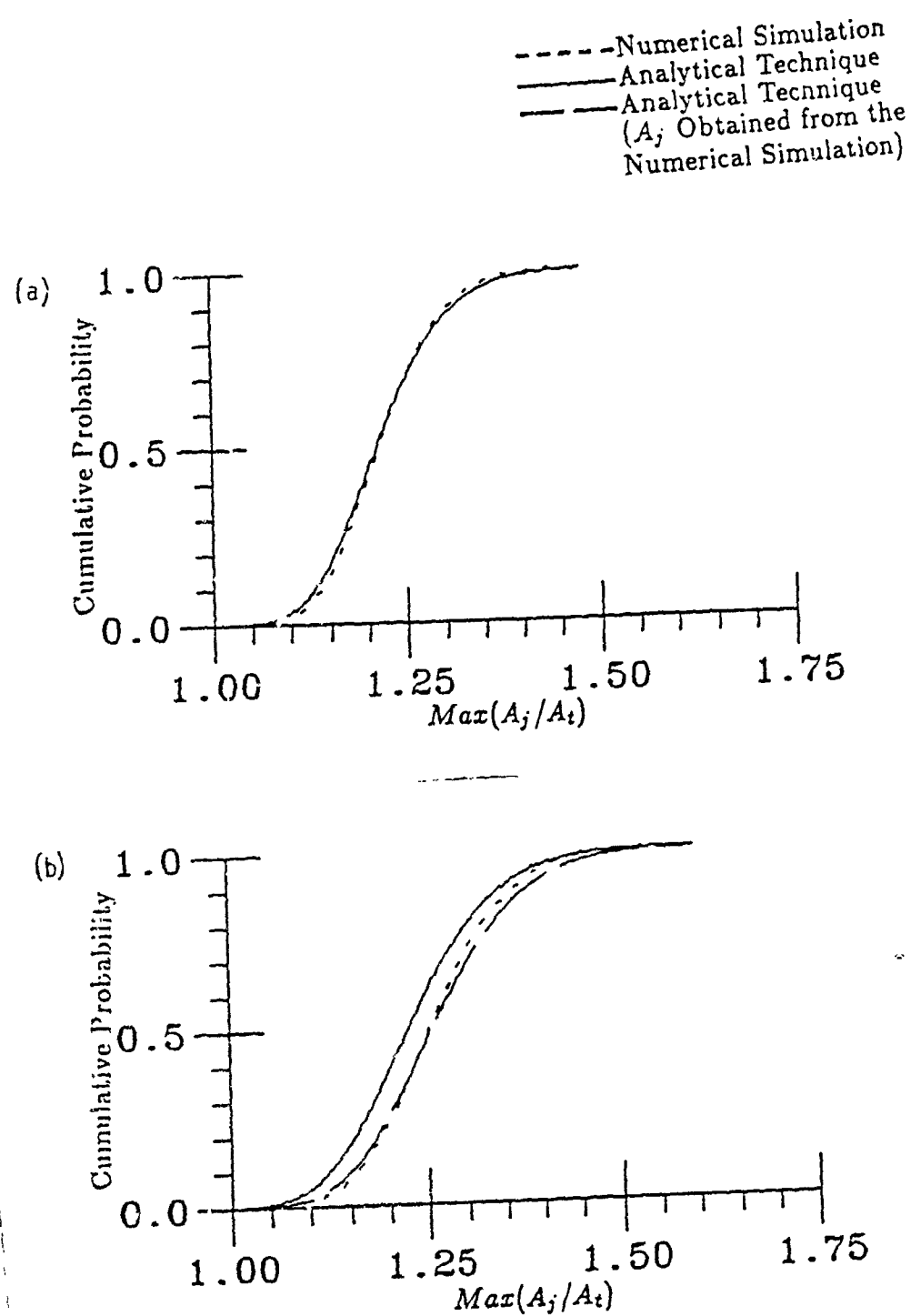


Figure 3 cdf of $\text{Max}(A_j/A_i)$: Numerical Simulation and Analytical Technique $N = 24$, $c = 1.443$, $\beta_r = 45^\circ$, (a) $\sigma_{\delta k j} = 7500$ (b) $\sigma_{\delta k j} = 10000$

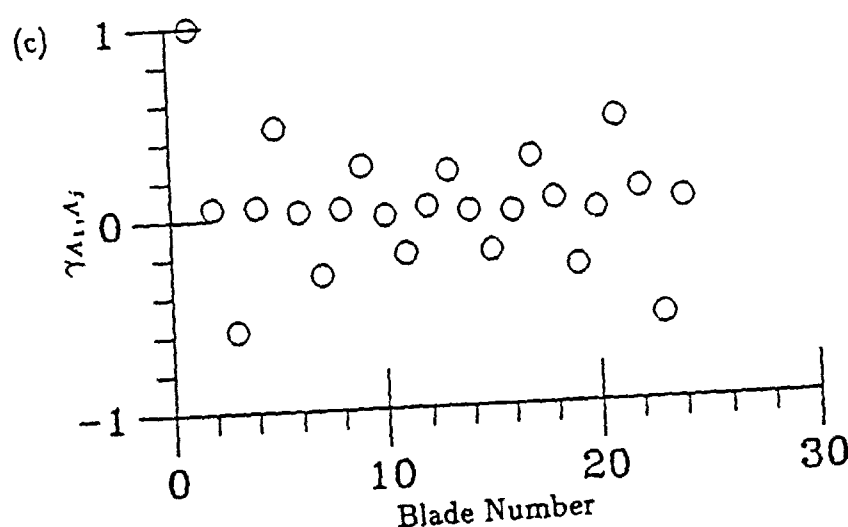
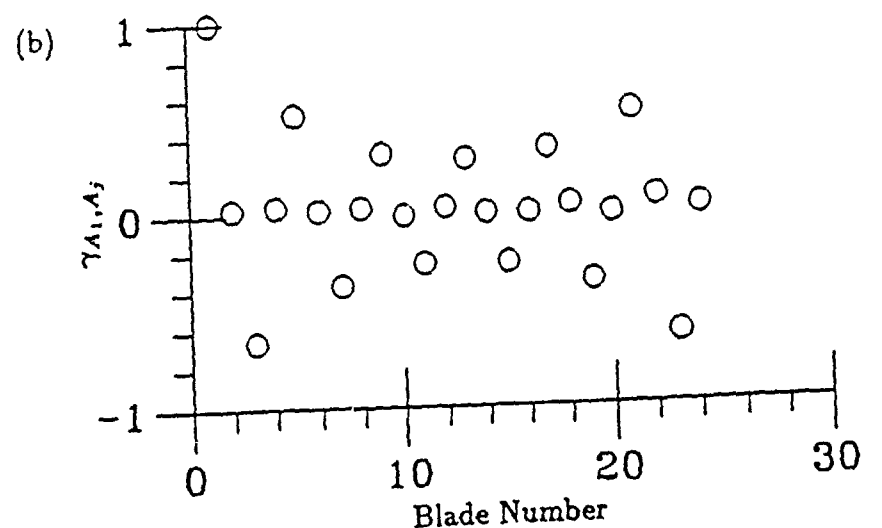


Figure 4 Correlation Coefficients, $\gamma_{A1,Aj}$
 $N = 24, c = 1.443, \beta_r = 45^\circ$
(a) $\sigma_{\delta k j} = 7500$ (b) $\sigma_{\delta k j} = 10000$

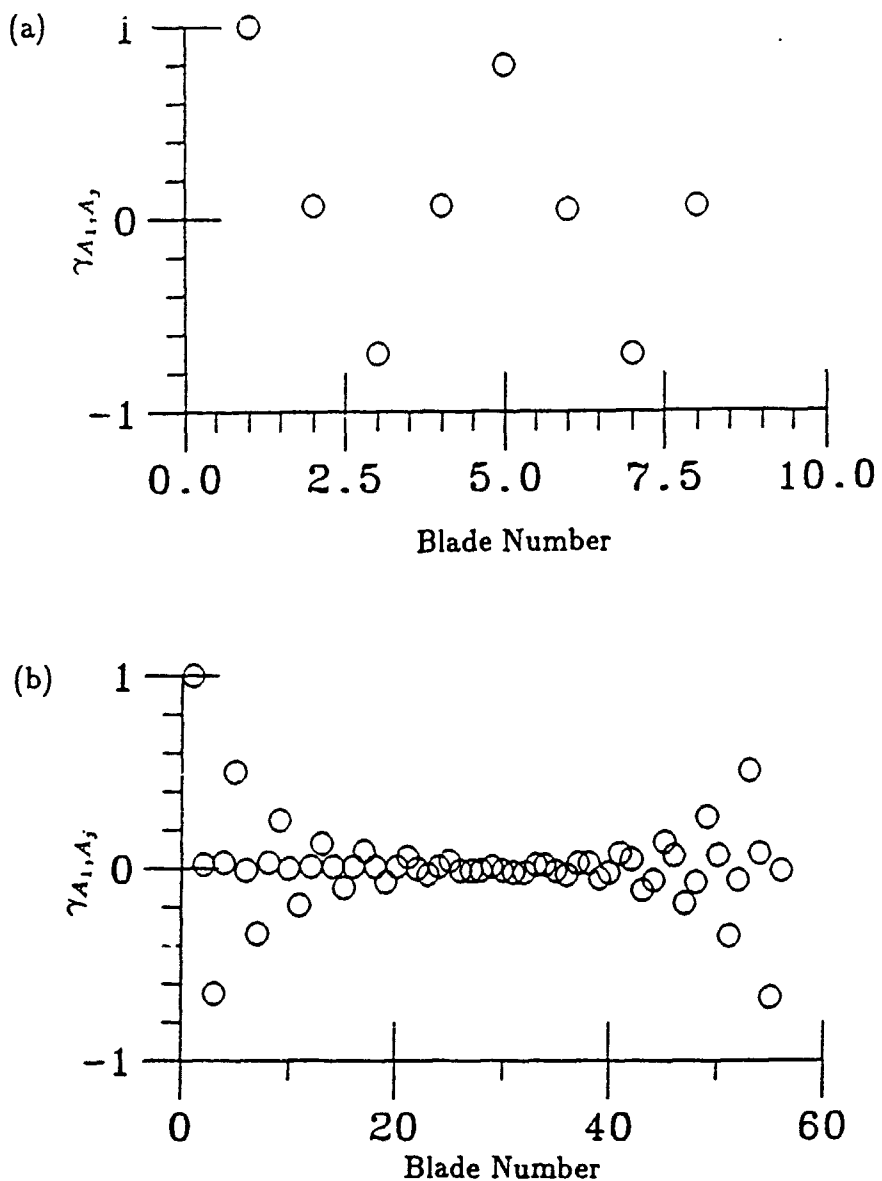


Figure 5. Correlation Coefficients, γ_{A_i, A_j} :
 $c = 1.443$, $\beta_r = 45^\circ$, $\sigma_{\delta k_j} = 7500 \delta k_j$: Gaussian
(a) $N = 8$ (b) $N = 56$

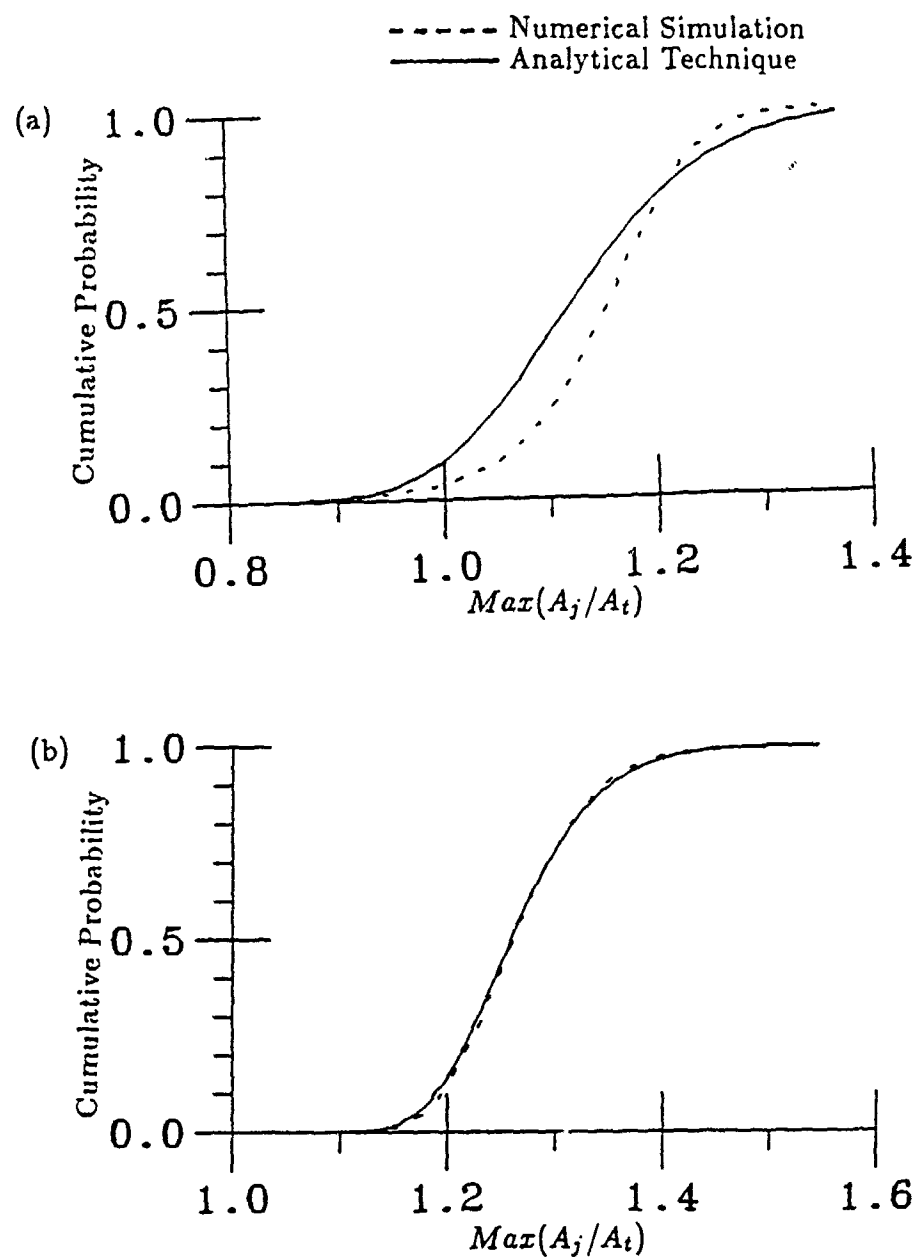


Figure 6. cdf of $\text{Max}(A_j/A_t)$
 Numerical Simulation and Analytical Technique
 $c = 1.443$, $\beta_r = 45^\circ$, $\sigma_{\delta k_j} = 7500 \delta k_j$: Gaussian
 (a) $N = 8$ (b) $N = 56$

SECTION 3
ANALYTICAL STATISTICS OF FORCED RESPONSE OF A MISTUNED
BLADED DISK ASSEMBLY IN SUBSONIC FLOW

Abstract

The statistics of the forced response of a structurally and aerodynamically coupled bladed disk assembly have been computed efficiently by the analytical technique. The validity of the analytical technique has been corroborated by comparison with the results from numerical simulations. Lastly, the effects of the following parameters on the statistics of the maximum amplitude have been studied: aerodynamic coupling, fluid density, and stagger angle.

Nomenclature

<u>Symbol</u>	<u>Meaning</u>
A_j	amplitude of x_j (mistuned system)
A_j^c	$= A_j \exp^{\theta_j}$
A_t	(resonant) amplitude of x_{tj} (tuned system)
b	semicord length
c	viscous damping (tuned system)
cdf	cumulative distribution function
$diag$	diagonal elements of a diagonal matrix
i	$\sqrt{-1}$
k_C	structural coupling stiffnesses between adjacent blades
k_j	modal stiffness of j^{th} blade (mistuned system)
k_t	modal stiffness of each blade (tuned system)
$\lambda_{whr}, \lambda_{hhr}$	nondimensional aerodynamic coefficients
m_t	modal mass of each blade (tuned system)
N	number of blades
S	spacing between adjacent blades
U	vector defined in equation (10)
V	velocity of fluid flow
x_j	response of j^{th} blade (mistuned system)

x_{tj}	response of j^{th} blade (tuned system)
α	stagger angle
β_r	interblade phase angle of r^{th} engine order
δk_j	$= k_j - k_t$
v	location of elastic axis
ω	excitation frequency (rad/sec)
ϕ_j	phase angle of x_j
ρ	fluid density
σ_y	standard deviation of random variable y
ζ	damping ratio

1. Introduction

Mistuning in a bladed disk assembly refers to the variation in the modal properties of blades because of manufacturing tolerances. It has received wide attention in the existing literature [1-5] because even a small amount of mistuning can lead to a large variation of blades' amplitudes within the same assembly. In fact, the amplitude of vibration of the worst blade may often be as high as one and one-half times the amplitude of a blade of a perfectly tuned system. Consequently, the fatigue life of a blade on a mistuned assembly may be significantly lower than that predicted on the basis of a perfectly tuned system. Furthermore, the deviations of the modal properties of blades from their nominal values are statistically distributed. As a result, there exists a large number of possible sets of blades' modal parameters that a bladed disk assembly can have. Since the maximum amplitude will be different for each such set of blades' modal parameters, it is important for the designer to know the statistics of the forced response, particularly the probability that the maximum amplitude on any disk would exceed a critical value in an efficient manner.

To study the dynamic response of a mistuned bladed disk assembly, the aerodynamic effects have been often simulated as constant viscous damping [6-11] associated with each blade's motion. This simple representation of aerodynamic forces provides a good basis for the development of physical concepts and mathematical techniques which are required to study the effects of mistuning on the forced response of a bladed disk assembly. However, this model does not consider certain important features of cascade aerodynamics, e.g., the aerodynamic coupling between each blade and the dependence of aerodynamic loads on the interblade phase angle, the frequency of blade motion, the Mach number, and various cascade parameters. The effect of limiting aerodynamic and structural coupling has been studied by Basu and Griffin [12], and the statistics of amplitudes were obtained by the numerical simulation. The aerodynamic coupling between each blade results in the dense system equations which require a large amount of computation to solve them. As a result, to generate the statistics of amplitudes by the

numerical simulation, the computational cost for an aerodynamically coupled system is much higher than that of a structurally coupled system. Consequently, the first objective here is to efficiently calculate the statistics of amplitudes of a mistuned assembly whose blades are coupled structurally and aerodynamically. Then, the next objective is to investigate the effects of various cascade parameters on the statistics of the amplitudes of a mistuned assembly.

The spring/mass model, Figure 1, is used in this paper to represent a rotor stage [6-11]. This model considers only one mode of vibration for each blade. The unsteady aerodynamic loads due to motions of blades in a rotor stage have been calculated by the linearized cascade theory [13-15] for the subsonic flow. For computing aerodynamic loads, the rotor stage is modeled as a two-dimensional cascade of blades, Figure 2. The blade is represented by a "typical section" motion which is assumed to vibrate in the bending mode, Figure 3.

In addition to the interblade phase angle ($\beta_r = 2\pi r/N$), the aerodynamic forces also depend on the stagger angle (α), the ratio of blade spacing to cord length ($S/2b$), the reduced velocity ($\omega b/V$), the Mach number, and the location of the elastic axis (v).

2. Governing Equations and Steady State Response

As stated in the Ref. [3] each blade has identical amplitude and the interblade phase angle is constant in each mode for the tuned cascade. Hence, for the r^{th} tuned mode, the response of the j^{th} blade, x_{ij} , can be represented as

$$x_{ij} = A_i^c \exp^{i(\beta_r + \omega t)} \quad (1)$$

where A_i^c is a complex number. Its magnitude represents the amplitude of motion. In a mistuned assembly for which each blade has a different response, the motion of the j^{th} blade, x_j , can be represented as a liner combination of all the tuned modes corresponding to all the interblade phase angles [3]; i.e.

$$x_j = \sum_{r=0}^{N-1} h_{ir} \exp^{i(\beta_r + \omega t)} = \sum_{r=0}^{N-1} h_{ir} \exp^{i(2\pi r j/N + \omega t)} \quad (2)$$

where h_{ar} are complex coefficients. Thus, for the mistuned assembly, the equation of motion for the j^{th} blade is [3]

$$m_j \ddot{x}_j + c \dot{x}_j + k_j x_j + kC(x_j - x_{j-1}) + kC(x_j - x_{j+1}) = L\pi\rho b^3 \omega^2 \sum_{r=0}^{N-1} \left[\lambda_{hhr} \frac{h_{ar}}{b} + \lambda_{whr} \right] \exp^{i(\omega t + \beta_r)} \quad (3)$$

where $j = 1, 2, \dots, N$. L and ρ are unit length and fluid density, respectively. The stiffnesses $k_j (= k_t + \delta k_j)$ are chosen as random variables to represent the mistuning in this study. The λ_{hhr} is the nondimensional lift coefficient [3] for the r^{th} tuned mode and λ_{whr} is the r^{th} nondimensional lift coefficient due to the wakes shed from upstream periodic obstructions. These nondimensional coefficients ($\lambda_{hhr}, \lambda_{whr}$) are obtained from the aerodynamic code, NASA Lewis Research Center [15]. The linear viscous coefficient, c , represents the damping from the structural sources. The value of the viscous damping coefficient, c , is selected so that the total damping in the tuned model is one percent of the system's critical damping which is usually found in practice [12].

For the steady state response, the motion of the j^{th} blade of the mistuned system can be represented as a harmonic motion

$$x_j = A_j^c \exp^{i\omega t} \quad (4)$$

where $A_j^c (= A_j \exp^{i\phi_j})$ is the complex amplitude. Comparing equations (2) and (4), one can obtain

$$A_j^c = \sum_{r=0}^{N-1} h_{ar} \exp^{i(2\pi r j / N)} \quad (5)$$

Then using the inverse discrete Fourier transformation [8], equation (5) yields

$$h_{ar} = \frac{1}{N} \sum_{j=1}^N A_j^c \exp^{-i(2\pi r(j-1) / N)} \quad (6)$$

Now substituting equations (4) and (6) into (3),

$$\begin{aligned} & (-m_j \omega^2 + ic\omega + k_j + 2kC + \delta k_j) A_j^c - kCA_{j-1}^c - kCA_{j+1}^c \\ & - \frac{L\pi\rho b^3 \omega^2}{N} \left\{ \sum_{s=1}^N \left[\sum_{r=0}^{N-1} \lambda_{hhr} \exp^{i(2\pi r(j-s+1) / N)} \right] A_s^c \right\} = L\pi\rho b^3 \omega^2 \sum_{r=0}^{N-1} \lambda_{whr} \exp^{i(2\pi r j / N)} \end{aligned} \quad (7)$$

The above equation can be written in the matrix form as follows

$$[H_A + \delta H] U = F_A \quad (8)$$

where the matrix H_A and the vector F_A are defined according to equation (7). And,

$$U = (A_1 \cos \phi_1, A_1 \sin \phi_1, \dots, A_N \cos \phi_N, A_N \sin \phi_N)^T \quad (9)$$

$$\delta H = \text{diag}(\delta k_1, \delta k_1, \delta k_2, \delta k_2, \dots, \delta k_N, \delta k_N). \quad (10)$$

In order to understand the nature of the mistuned response, the wake excitation (λ_{whr}) in one particular engine order will be considered at a time throughout this study. As one can see in equation (7), the motion of each blade is coupled to all the blades by the aerodynamical terms which result in the dense system equation. Consequently, the computation time for the numerical simulation gets enhanced.

For a tuned system ($\delta k_j = 0$ and $A_j^c = A_m^c \exp^{i2\pi(j-m)/N}$ [3]) under the r^{th} engine order excitation, equation (7) can be simplified as follows:

$$[-m_r \omega^2 + k_r + 2kC(1 - \cos(2\pi r/N)) - L\pi\rho b^2 \omega^2 \lambda_{hhr} + i\omega c] A_r^c = L\pi\rho b^3 \omega^3 \lambda_{whr} \exp^{i2\pi r/N}. \quad (11)$$

The resonant frequency (ω_r) and the damping ratio (ζ) of the tuned system can be computed as follows:

$$\omega_r = \left[\frac{k_r + 2kC(1 - \cos(2\pi r/N))}{m_r + L\pi\rho b^2 \text{Re} \lambda_{hhr}} \right]^{\frac{1}{2}}, \quad (12)$$

$$\zeta = \frac{c - \pi\rho b^2 \omega_r \text{Im} \lambda_{hhr}}{2(m_r + L\pi\rho b^2 \text{Re} \lambda_{hhr}) \omega_r}. \quad (13)$$

3. Analytical Technique to Compute the Statistics of Blades' Amplitudes

Even though the system with aerodynamic coupling is more complicated than that with only structural coupling, it still remains linear. Hence, the analytical technique developed in Ref [11] can be directly applied to compute the statistics of blades' amplitudes: the mean, the variance and the cdf of an amplitude, the correlation coefficients between any two amplitudes, and the cdf of the maximum amplitude on a rotor stage. Therefore, the objective here is to

study the accuracy of this technique and the aerodynamic effects on the statistics of the maximum amplitude.

4. Comparison with the Numerical Simulation

To verify the applicability of the analytical techniques to the mistuned systems with structural and aerodynamical coupling between blades, the cdf of $\text{Max}(A_j/A_t)$ from the analytical technique [11] is compared with that from the numerical simulation, where A_t is the resonant amplitude of the tuned system. For the numerical simulation, the IMSL subroutine DRNNOA [16] is used to choose the modal stiffnesses (δk_j) from the Gaussian population with $E[\delta k_j] = 0$ and $\sigma_{\delta k_j} = 7500$ Newton/meter. The response of the resulting bladed disk assembly is obtained by solving the N linear algebraic equations (7) in terms of $A_j \exp^{i\Phi_j}$ with the IMSL subroutine DL2LCG [16]. The cdf of $\text{Max}(A_j/A_t)$ of each blade is then generated by considering a large number (arbitrarily chosen to be 3000) of bladed disk assemblies with different sets of blades' modal stiffnesses. The nominal values of the system parameters are shown in Table 1, where the aerodynamic parameters are chosen from Ref. [3]. The engine order of excitation is chosen to be seven; i.e. $r = 7$. The amount of damping from the aerodynamic source in the tuned model is found to be 0.78 percent of the system's critical damping under the seventh engine order excitation. Hence, the value of the viscous damping coefficient, c , has been chosen to be 0.22 percent of the critical damping; i.e. $c = 0.3193$ Newton-sec/meter. Since the semicord length, b , on the right hand side of equation (7) acts as a scaling factor, it is chosen to be unity in this study.

In Figure 4, the cdf of $\text{Max}(A_j/A_t)$ from the analytical technique [3] agrees well with that from the numerical simulation. This result indicates that the analytical technique developed in Ref [11] can also efficiently and accurately compute the statistics of blades' amplitudes of a mistuned assembly whose blades are coupled structurally and aerodynamically.

5 Parametric Studies

5.1 The Effect of Aerodynamic Couplings Among Blades

The statistical response of the system developed in Ref. [11] whose blades are only coupled structurally with the immediate neighbours is compared with that of the system developed in this paper. In each system, the equivalent viscous damping ration (ζ) is equal to 1.0%. The cumulative distribution functions of $\text{Max}(A_j/A_1)$ indicate that the aerodynamically coupled system has a higher probability of having a larger amplitude, Figure 5. These results indicate that the system in which the aerodynamic effects are modeled as a viscous damping associated with each blade's motion underestimates the effects of mistuning.

5.2 The Effect of Fluid Density

From equation (7), it is clear that the fluid density controls the aerodynamic damping and the coupling between blades. The statistics of amplitudes are computed for the following values of the fluid density: 0.75 ρ_0 , ρ_0 , 1.25 ρ_0 and 1.5 ρ_0 . The cdf of $\text{Max}(A_j/A_1)$ for each value of the fluid density is shown in Figure 6. It indicates that the system with a larger value of the fluid density has a smaller probability of having a higher amplitude. In other words, the impact of mistuning is more severe on the system with a lower value of the fluid density.

5.3 The Effect of Stagger Angle

The aerodynamic coefficients (λ_{hhr} and λ_{whr}) depend on the stagger angle of the cascade (Figure 2). As a result, the aerodynamic damping and the coupling between blades will be different for each stagger angle. The statistics of amplitudes are computed for the following values of the stagger angle (α): 15°, 30°, 45°, 60° and 75°. Even though the variation in the equivalent viscous damping ration (ζ) is large for these stagger angles ($\zeta=0.80\%$, 0.83%, 0.91%, 1.08%, 1.54% for $\alpha=15^\circ$, 30°, 45°, 60° and 75°, respectively), the results, cdf of $\text{Max}(A_j/A_1)$, indicate the the statistics of the blades' amplitudes are not highly sensitive to the variation in the stagger angle, Figure 7.

From the above results, it is clear that the damping ratio alone, which only depends on λ_{hhr} , equation (13), is not enough to explain the mistuning effect. The effect of other aerodynamic coupling terms ($\lambda_{h,hj}, j \neq r$) should be considered as well. To consider the impact of these terms, one can compute the inverse value of the condition number (τ) of the system matrix, H_A . The inverse value of the condition number can measure how close a matrix is to the singularity [17]. The smaller the value of τ is, the closer is the matrix to the singularity, and the higher order terms will be consequently more important. The values of τ for the system matrix with stagger angle $\alpha=15^\circ, 30^\circ, 45^\circ, 60^\circ$ and 75° , are 0.04356, 0.04385, 0.04471, 0.04676, and 0.0445, respectively. The results indicate that the degree with which each system is close to the singularity is almost the same. Consequently, the statistical distribution of amplitudes are identical in spite of the variation in the equivalent viscous damping for the r^{th} tuned mode.

In section 5.1, $\tau=0.05878$ for the structurally coupled system [11], while $\tau=0.04596$ for the aerodynamically coupled system. Therefore, even though the total damping ratio is 1% for the r^{th} tuned mode in each case, the scatter in amplitudes of the aerodynamically coupled system is greater than that of the structurally coupled system (Figure 5).

In section 5.2, $\tau=0.0383, 0.04596, 0.05319$ and 0.06 for the fluid density equal to $0.5 \rho, \rho, 1.25\rho$, and 1.5ρ , respectively. And, the corresponding equivalent viscous damping ratios are 0.80%, 1.00%, 1.20% and 1.39%, respectively. Therefore, the system matrix is less singular and the equivalent viscous damping ratio also increases as the fluid density increases. These facts explain why the system is less sensitive to mistuning as the fluid density increases (Figure 6).

6. Conclusions

The statistics of the forced response have been computed by the analytical technique [11] for a linear assembly whose blades are coupled structurally and aerodynamically. The validity of the analytical technique has been corroborated by comparison with the results from the

numerical simulation. The CPU time for the analytical technique is found to be much smaller than that for the numerical simulation. On a VAX 8550 computer, the CPU times for the numerical simulation and the analytical technique are 3068.0 seconds and 9.72 seconds, respectively.

The parametric studies indicate the following:

- 1) The mistuning effect on a blade's amplitude may be underestimated by the structurally coupled system in which the aerodynamic effects are modeled as a viscous damping associated with each blade.
- 2) The probability of having a blade with a larger amplitude decreases as the fluid density increases.
- 3) The stagger angle of the cascade has little impact on the statistics of a blade's amplitude under the subsonic flow condition.

References

- [1] Whitehead, D. S., "Effect of Mistuning on the Vibration of Turbomachine Blades Induced by Wakes," *Journal of Mechanical Engineering Science*, Vol. 8, No. 1, 1966, pp. 15-21.
- [2] Ewins, D. J., "Vibration Characteristics of Bladed Disc Assemblies," *Journal of Mechanical Engineering Science*, Vol. 15, No. 3, 1973, pp. 165-186.
- [3] Kaza, K. R. V. and Kielb, R. E., "Flutter and Response of Mistuned Cascade in Incompressible Flow," *AIAA Journal*, Vol. 20, No. 8, August 1982, pp. 1120-1127.
- [4] Kielb, R. E. and Kaza, K. R. V., "Aeroelastic Characteristics of a Cascade of Mistuned Blades in Subsonic and Supersonic Flows," *ASME Paper No. 81-DET-122*, September 1981.
- [5] Kielb, R.E., Crawley, E., and Simonis, J.C. (Editors), Bladed Disk Assemblies, ASME DE - Vol. 6, 1987.
- [6] Griffin, J. H. and Hoosac, T. M., "Model Development and Statistical Investigation of Turbine Blade Mistuning," *Journal of Vibration, Acoustics, Stress and Reliability in Design*, Vol. 106, April 1984, pp. 204-210.
- [7] Sinha, A., "Calculating the Statistics of Forced Response of a Mistuned Bladed Disk Assembly," *AIAA Journal* Vol. 24, No. 11, 1986, pp. 1797-1801.
- [8] Sinha, A. and Chen, S., "Probabilistic Analysis of Forced Response of a Mistuned Bladed Disk Assembly with Various Mistuning Distributions," *AIAA paper #88-2399, Proceedings of the 29th AIAA/ASME/ASCE/AHS Structures, Structural Dynamics and Materials Conference*, April 1988, pp. 1487-1496.
- [9] Sinha, A. and Chen, S., "A Higher-Order Technique to Calculate the Statistics of Forced Response of a Mistuned Bladed Disk Assembly," *Journal of Sound and Vibration*, April 1989.
- [10] Chen, S. and Sinha, A., "Calculating the Statistics of Forced Response of a Mistuned Bladed Disk Assembly with Friction Dampers," submitted to *ASME Journal of Vibration and Acoustics*
- [11] Chen, S. and Sinha, A., "Calculating the Statistics of Maximum Amplitude of a Bladed Disk Assembly," to be submitted to *Journal of Sound and Vibration* (also, section 2 of this report).
- [12] Basu, P. and Griffin J. H., "The Effect of Limiting Aerodynamic and Structural Coupling in Models of Mistuned Bladed Disk Vibration," *Journal of Vibration, Acoustics, Stress, and Reliability in Design*, Vol. 108, April 1986, pp. 132-139.
- [13] Smith, S. N., "Discrete Frequency Sound Generation in Axial Flow Turbomachines," *Aeronautical Research Council, Reports and Memoranda*, No. 3709, University of Cambridge, Cambridge, England, 1973.

- [14] Rao, B. M. and Jones, W. P., "Unsteady Airloads on a Cascade of Staggered Blades in Subsonic Flow," 46th Propulsion Energetics Review Meeting, Monterey, California, September 1975, AGARD-CP-177.
- [15] Rao, B. M., "Fortran Computer Program: Calculating Aerodynamic Coefficients in Subsonic Flow," NASA Lewis Research Center, Cleveland.
- [16] IMSL Reference Manual, IMSL, Inc., Houston, TX, 1987.
- [17] Klema, V.C. and Laub, A.J., "The Singular Value Decomposition: Its Computation and Some Applications," IEEE Transactions on Automatic Control, Vol. AC-25, No. 2, April 1980, pp. 164-176.

Table 1: Data for Simulation -- Aerodynamically Coupled System (SI Unit)

$m_t/(L\pi\rho b^2) = 258.5$	$M = 0.7$
$\omega b/V = 0.55$	$\alpha = 54^\circ$
$v = 0.5$	$S/(2b) = 0.534$
$m_t = 0.0114$	$k_C = 45430.0$
$k_t = 430000$	$N = 56$
$c = 0.3193$	$\sigma_{\delta k_j} = 7500.0$
$E[\delta k_j] = 0$	δk_j : Gaussian

c : viscous damping from structural source only

All the blades are aerodynamically coupled, equation (7).

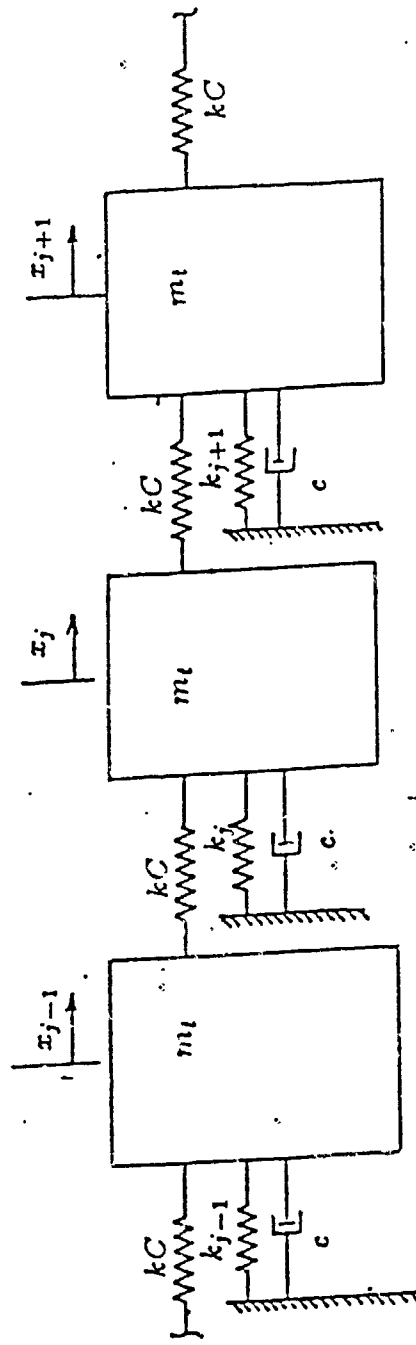


Figure 1. Spring/Mass Model of a Rotor Stage (Linear System)

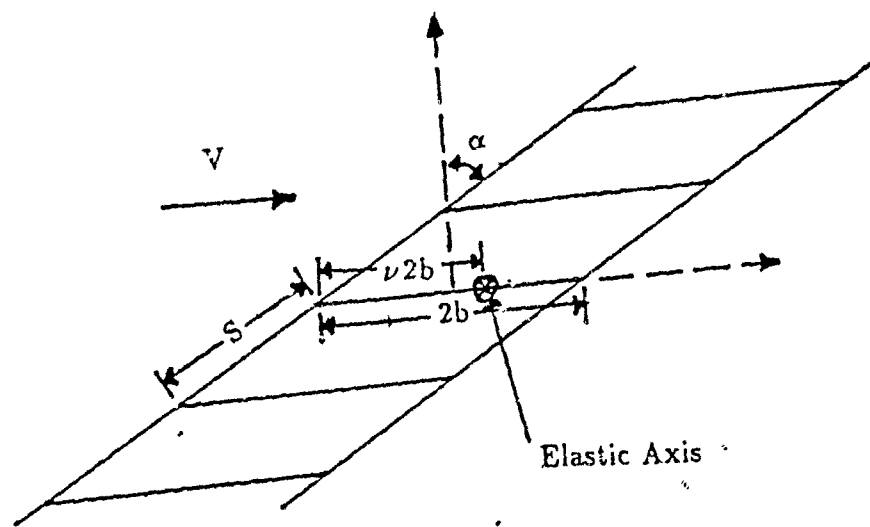


Figure 2. Cascade of Blades

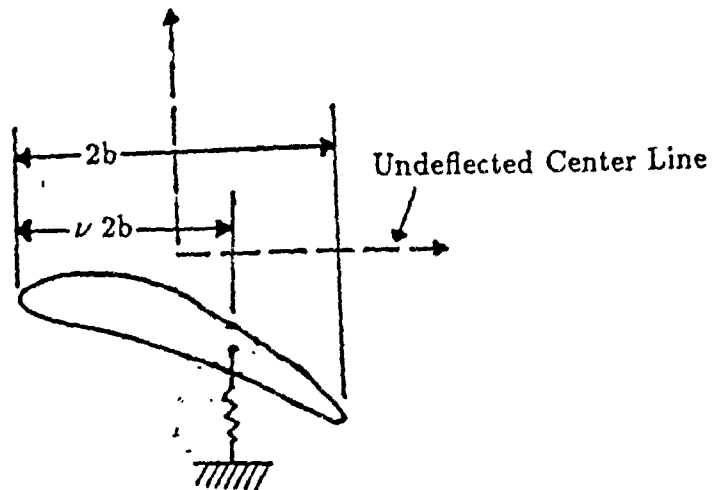


Figure 3. Equivalent Section of a Blade

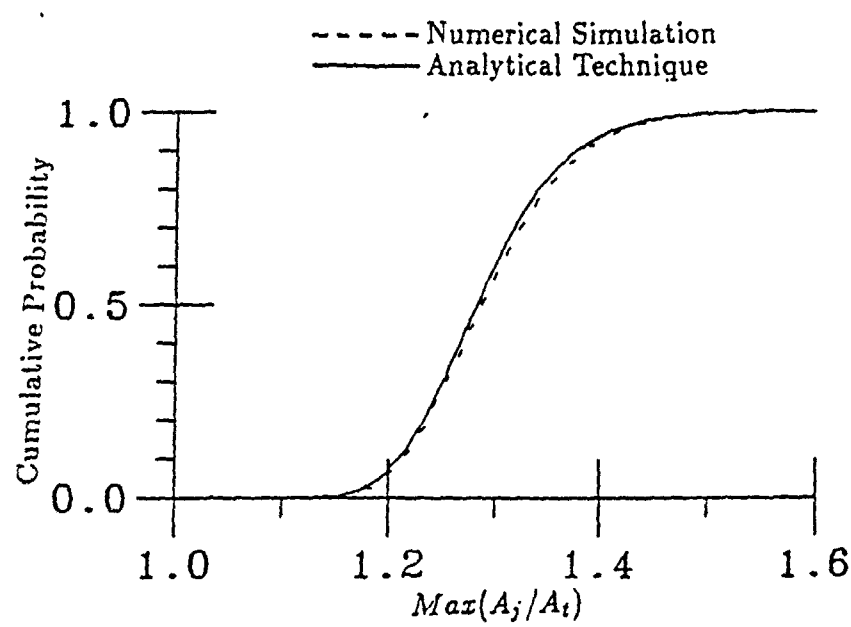


Figure 4. cdf of $\text{Max}(A_j/A_t)$
Numerical Simulation and Analytical Technique
 $N = 56$, $c = 0.3193$, $\beta_r = 45^\circ$, $\sigma_{\delta k_j} = 7500$, δk_j : Gaussian

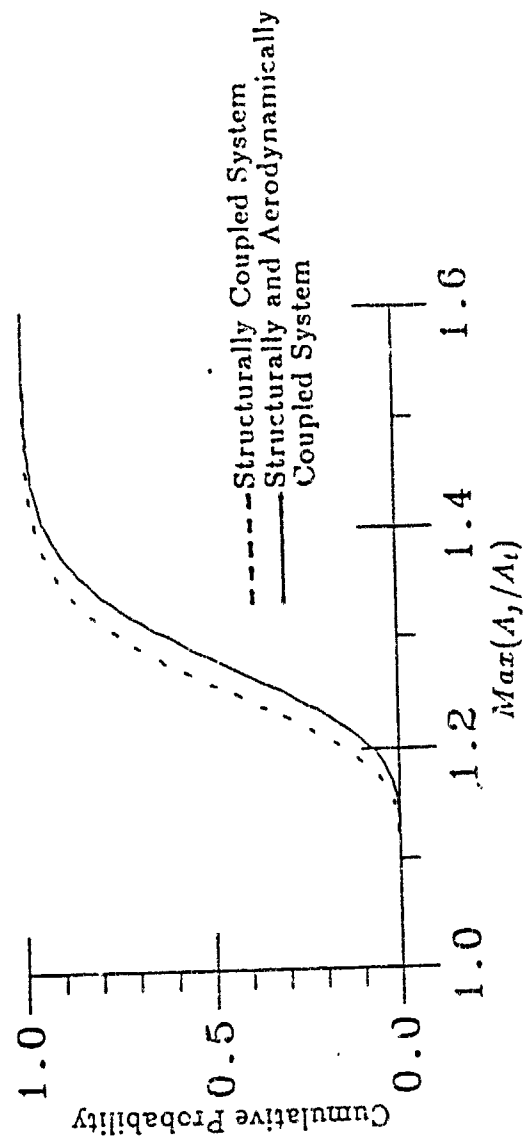


Figure 5. The Effect of the Aerodynamic Coupling on the cdf of $\text{Max}(A_j/A_i)$
 $N = 56$, $\beta_r = 45^\circ$, $\sigma_{6k_j} = 7500$, δk_j : Gaussian

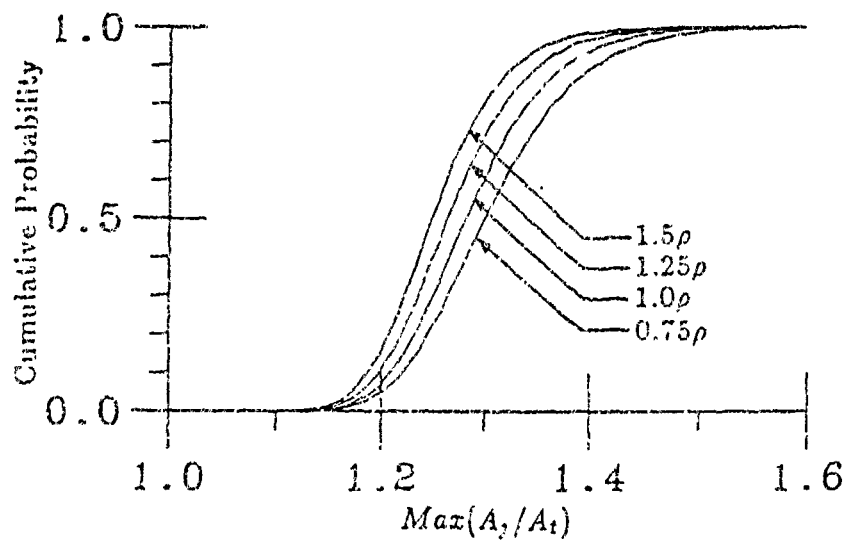


Figure 6. The Effect of Fluid Density
on the cdf of $\text{Max}(A_j/A_t)$
 $N = 56$, $c = 0.3193$, $\beta_r = 45^\circ$, $\sigma_{\delta k_j} = 7500$, δk_j : Gaussian

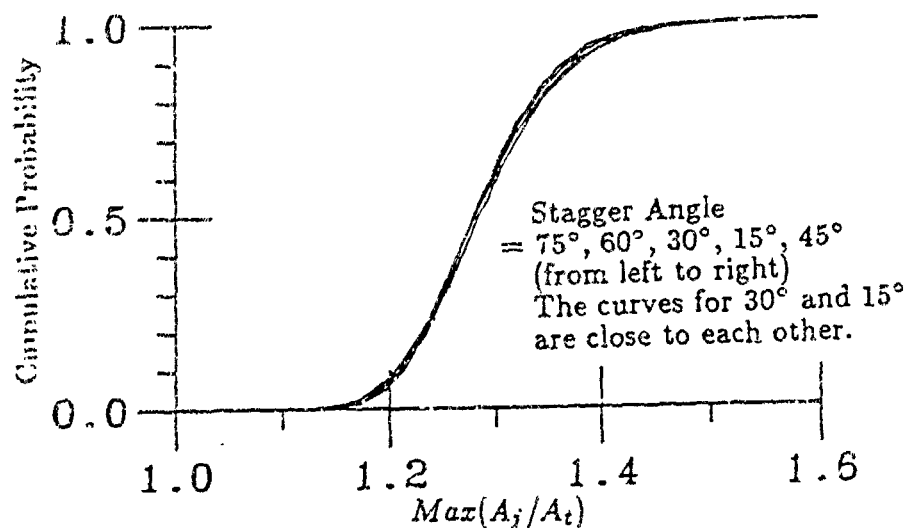


Figure 7. The Effect of Stagger Angle
on the cdf of $\text{Max}(A_j/A_t)$
 $N = 56$, $c = 0.3193$, $\beta_r = 45^\circ$, $\sigma_{\delta k_j} = 7500$, δk_j : Gaussian